LETTER

doi:10.1038/nature25442

Monitoring T cell–dendritic cell interactions *in vivo* by intercellular enzymatic labelling

Giulia Pasqual[1], Aleksey Chudnovskiy[1], Jeroen M. J. Tas[1], Marianna Agudelo[1], Lawrence D. Schweitzer[2,3], Ang Cui[2,3], Nir Hacohen[2,3] & Gabriel D. Victora[1]

Interactions between different cell types are essential for multiple biological processes, including immunity, embryonic development and neuronal signalling. Although the dynamics of cell–cell interactions can be monitored *in vivo* by intravital microscopy[1], this approach does not provide any information on the receptors and ligands involved or enable the isolation of interacting cells for downstream analysis. Here we describe a complementary approach that uses bacterial sortase A-mediated cell labelling across synapses of immune cells to identify receptor–ligand interactions between cells in living mice, by generating a signal that can subsequently be detected *ex vivo* by flow cytometry. We call this approach for the labelling of 'kiss-and-run' interactions between immune cells 'Labelling Immune Partnerships by SorTagging Intercellular Contacts' (LIPSTIC). Using LIPSTIC, we show that interactions between dendritic cells and CD4$^+$ T cells during T-cell priming *in vivo* occur in two distinct modalities: an early, cognate stage, during which CD40–CD40L interactions occur specifically between T cells and antigen-loaded dendritic cells; and a later, non-cognate stage during which these interactions no longer require prior engagement of the T-cell receptor. Therefore, LIPSTIC enables the direct measurement of dynamic cell–cell interactions both *in vitro* and *in vivo*. Given its flexibility for use with different receptor–ligand pairs and a range of detectable labels, we expect that this approach will be of use to any field of biology requiring quantification of intercellular communication.

LIPSTIC is based on proximity-dependent labelling across cell–cell interfaces using the *Staphylococcus aureus* transpeptidase sortase A (SrtA). SrtA covalently transfers a substrate containing the sorting motif 'LPXTG' to a nearby N-terminal oligoglycine[2] (Extended Data Fig. 1). For LIPSTIC, a ligand and receptor of interest are genetically fused to either SrtA or a tag that consists of five N-terminal glycine residues (G5). Addition of a SrtA substrate (for example, an LPETG peptide linked at the N terminus to a detectable label, such as biotin or a fluorophore) leads to loading of this peptide onto SrtA on the donor cell via the formation of an acyl intermediate. When a ligand and receptor interact, SrtA catalyses the transfer of the substrate onto the G5-tagged receptor. After cells separate, the interaction history is revealed by the presence of the label on the surface of the G5-expressing cell (Fig. 1a). To ensure that labelling occurs specifically as a readout of the ligand–receptor interaction—rather than being driven by the affinity of SrtA to G5—we used an engineered SrtA variant with a 13-fold lower affinity for G5 compared to wild-type SrtA (K_m of engineered SrtA = 1,830 ± 330 μM compared to a K_m = 140 ± 30 μM for wild-type SrtA)[3]. This affinity is orders of magnitude lower than most receptor–ligand interactions involved in immune function[4–7].

To test this system, we transfected two populations of HEK293T cells separately with either G5–CD40 or CD40L–SrtA, mixed the two populations in the presence of the biotinylated SrtA substrate (biotin–LPETG) for 30 min, and then analysed the cells by flow cytometry and western blot. To determine specificity, G5–CD40 cells were also incubated with HEK293T cells transfected with SrtA fused to a CD40L variant carrying two point mutations that strongly impair binding to CD40[8,9] (CD40L*–SrtA, Extended Data Fig. 2) or with untargeted SrtA anchored to the cell surface by the transmembrane domain of PDGFR (SrtA–PDGFR) (Fig. 1b, c). Flow cytometric analysis showed that G5–CD40$^+$ cells were biotinylated efficiently only when incubated with cells expressing wild-type CD40L–SrtA (Fig. 1d). Western blotting confirmed that LIPSTIC labelling occurred via covalent modification of G5–CD40 (Fig. 1e). Specific intercellular labelling was also achieved with other ligand–receptor pairs that are involved in immune cell interactions and neuronal signalling, indicating that LIPSTIC can be used to analyse a variety of molecular interactions (Fig. 1f–h). To visualize the dynamics of LIPSTIC labelling *in vitro*, we imaged interactions between B cells transduced with G5–CD40 and CD4$^+$ T cells transduced with CD40L–SrtA and preloaded with Alexa Fluor 647–LPETG. Substrate transfer between T and B cells was observed within minutes of interaction and at the interacting surface (Extended Data Fig. 3 and Supplementary Video 1). We conclude that LIPSTIC is an efficient, specific and versatile method that is able to label receptor–ligand interactions across cells *in vitro*, suitable for use with multiple receptor–ligand pairs and for detection by both flow cytometry and microscopy.

To determine whether LIPSTIC can function *in vivo* and at endogenous levels of receptor and ligand expression, we generated mice carrying *Cd40*^{G5} and *Cd40lg*^{SrtA} alleles targeted to their endogenous loci (Extended Data Fig. 4). Expression of G5–CD40 was made constitutive, whereas expression of CD40L–SrtA was designed to occur only after Cre-mediated excision of a translational stop cassette, in order to specify the SrtA$^+$ donor cell population. To measure LIPSTIC labelling during antigen-specific interactions between T cells and antigen-presenting cells, we crossed *Cd40lg*^{SrtA} to CD4-Cre and to OT-II TCR mice, which express a T-cell receptor specific for the chicken ovalbumin (OVA) peptide OVA$_{323–339}$ (we refer to this strain as OT-II–SrtA). We co-cultured OT-II–SrtA CD4$^+$ T cells for 6 h with *Cd40*$^{G5/G5}$ splenic dendritic cells treated either with OVA$_{323–339}$ or with a control LCMV-GP$_{61–80}$ peptide and added the biotinylated substrate during the final 20 min of culture (Fig. 2a). Efficient intercellular labelling only occurred when dendritic cells were treated with the cognate peptide, which correlated with induction of CD40L–SrtA expression on T cells. Dendritic cell labelling was strongly inhibited by addition of a CD40L-blocking antibody, confirming that the CD40–CD40L interaction is required (Fig. 2b, c). LIPSTIC labelling was dose-responsive over a six-log range of OVA peptide concentrations (Fig. 2d, e). Co-culture of OT-II–SrtA CD4$^+$ T cells with two *Cd40*$^{G5/G5}$ dendritic cell populations separately pulsed with either the OVA$_{323–339}$ or control LCMV-GP$_{61–80}$ peptide showed that labelling was restricted to dendritic cells loaded with the cognate antigen, also across a wide range of antigen doses (Fig. 2f–h). Whereas labelling of cognate dendritic cells increased

[1]Laboratory of Lymphocyte Dynamics, The Rockefeller University, 1230 York Avenue, New York, New York, USA. [2]Broad Institute of MIT and Harvard, Cambridge, Massachusetts, USA. [3]Center for Cancer Research, Massachusetts General Hospital, Department of Medicine, Boston, Massachusetts, USA.

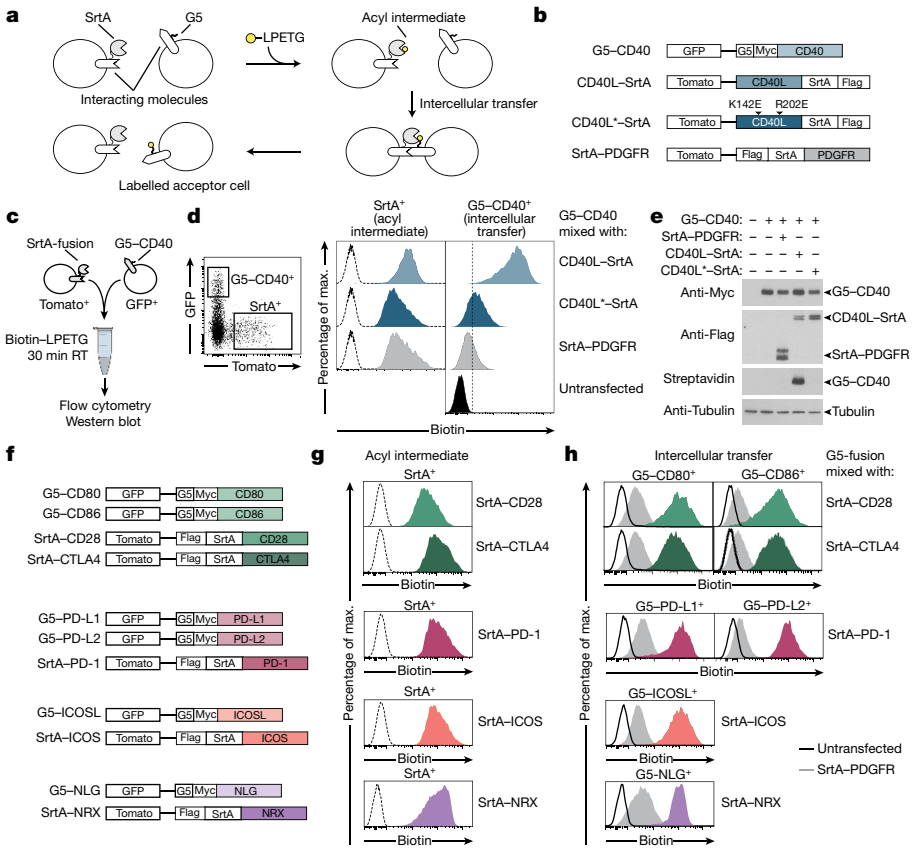

Figure 1 | Using LIPSTIC to track ligand–receptor interactions. **a**, Schematic representation of the LIPSTIC approach. **b**, Constructs used in **c**–**e**. All constructs express a bicistronic gene that encodes a fluorescent reporter protein. **c**, Experimental setup to analyse intercellular labelling in transfected HEK293T cells. RT, room temperature. **d**, Gating strategy and histograms showing biotin staining in SrtA$^+$ cells (left column, indicating the formation of the acyl intermediate) and G5–CD40$^+$ cells (right column, indicating intercellular transfer). Histograms with dashed lines represent untransfected cells. **e**, Western blot showing expression of G5–CD40 (anti-Myc), SrtA fusion constructs (anti-Flag) and intercellular labelling (Streptavidin). Tubulin is used as a loading control. **f**, Constructs used in **g**, **h**. NLG, neuroligin; NRX, neurexin. **g**, **h**, Biotin staining in SrtA$^+$ cells (acyl intermediate) and G5$^+$ cells (intercellular transfer). Histograms with dashed lines represent untransfected cells. Histograms with solid lines and grey histograms represent G5$^+$ cells mixed with untransfected and SrtA–PDGFR donor cells, respectively. Data are representative of three independent experiments.

when the substrate was incubated for a longer time, labelling of control dendritic cells was negligible even when the substrate was present for the full 6 h of co-culture (Extended Data Fig. 5a–c). LIPSTIC was also capable of specifically identifying B cells that were productively engaged with antigen, as determined by co-culture of antigen-specific and polyclonal B cells with OT-II–SrtA CD4$^+$ T cells (Extended Data Fig. 5d–g). Therefore, LIPSTIC labelling in short-term *ex vivo* priming experiments is dependent on interactions between receptor and ligand, dose-responsive across a wide range of antigen concentrations, and specific to target cells displaying cognate antigens. Of note, although SrtA–CD40L was capable of stimulating B-cell activation when expressed on HEK293T cells (Extended Data Fig. 2c), B-cell activation by CD40L–SrtA CD4$^+$ T cells was impaired both *ex vivo* and *in vivo* when compared to activation by T cells expressing wild-type CD40L, indicating that signalling by CD40L is partly compromised (Extended Data Fig. 6a, b). This impairment was also seen in mice not carrying the CD4-Cre transgene, which expressed a construct that only had a translated LoxP site added to the C terminus of CD40L (Extended Data Fig. 6b); this impairment therefore more likely represents a specific feature of the CD40L molecule than a general property of SrtA-fusion proteins. Nevertheless, experiments using dendritic cells as antigen-presenting cells showed no measurable effect of the *Cd40lg*^{SrtA} allele on T-cell proliferation, indicating that the overall kinetics of T-cell priming are not affected by CD40L insufficiency (Extended Data Fig. 6c); we therefore used interactions between T cells and dendritic cells to characterize LIPSTIC labelling *in vivo*.

To determine whether LIPSTIC can be used *in vivo*, we used a well-established T-cell priming model in which OVA$_{323–339}$-treated *Cd40*$^{G5/G5}$ dendritic cells were injected subcutaneously into the footpad of recipient mice, followed 18 h later by intravenous transfer of OT-II–SrtA CD4$^+$ T cells[10]. We delivered the LIPSTIC substrate to the popliteal lymph node (PLN) by footpad injection of a total of 300 nmol of biotin–LPETG over six injections between 10 and 12 h after T-cell transfer (Fig. 3a); T cells are engaged in long-lived interactions with antigen-bearing dendritic cells at this time, as determined by intravital imaging[10]. Flow cytometry of PLN cells showed efficient LIPSTIC labelling of transferred dendritic cells, which was dependent on T-cell expression of CD40L–SrtA and sensitive to treatment with a CD40L-blocking antibody (Fig. 3b, c and Extended Data Fig. 7a). Background labelling was negligible in all assayed cell populations (Extended Data Fig. 7b). To further confirm the dependence of LIPSTIC labelling on CD40–CD40L interaction, we took advantage of the observation that, in the absence of a *Cd40*^{G5} allele, endogenous N-terminal glycines on the cell surface can function as low-efficiency acceptors for the SrtA substrate[11] (Extended Data Fig. 7c, d). Such labelling was completely absent when Ag-loaded dendritic cells were deficient in *Cd40*, again showing that CD40–CD40L engagement is essential for labelling (Extended Data Fig. 7e, f). Analysis of the kinetics of substrate clearance from labelled cells showed that a fraction of the label was still detectable at 4 and 8 h after substrate injection (Extended Data Fig. 7g–k).

To measure the interaction between CD4$^+$ T cells and endogenous dendritic cells after immunization, we adoptively transferred

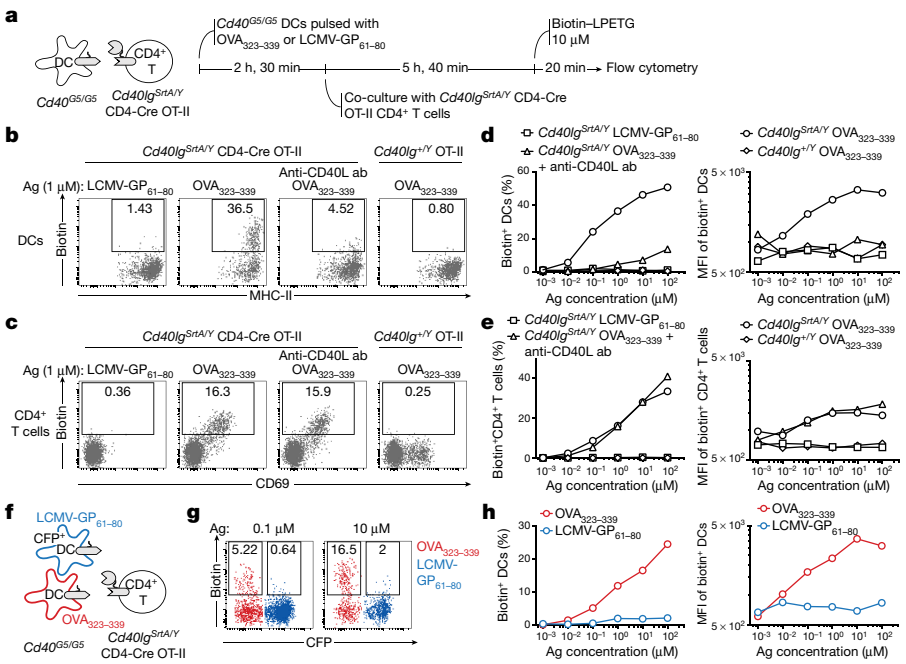

Figure 2 | LIPSTIC labelling of CD40–CD40L interactions *ex vivo*. **a**, Experimental setup for **b**–**e**. *Cd40lg*$^{SrtA/Y}$, male mice with only one copy of the *Cd450lg*^{SrtA} allele (*Cd40lg* is an X-chromosome-linked gene). **b**, Flow cytometry for biotin labelling of dendritic cells treated with 1 μM of the indicated peptide (intercellular transfer). **c**, Flow cytometry for biotin labelling of CD4$^+$ T cells (acyl intermediate). **d**, **e**, Percentage (left) and median fluorescence intensity (MFI, right) of biotin$^+$ dendritic cells (**d**) and CD4$^+$ T cells (**e**). **f**, Experimental setup for **g**, **h**; timeline as in **a**. **g**, Flow cytometric analysis of dendritic cells treated with 0.1 or 10 μM of the indicated peptides showing biotin labelling (intercellular transfer). **h**, Percentage (left) and MFI (right) of biotin$^+$ dendritic cells gated as in **g**. All data are representative of three independent experiments.

OT-II–SrtA CD4$^+$ T cells into *Cd40*$^{G5/G5}$ hosts and performed *in vivo* LIPSTIC labelling at different times after footpad injection of 10 μg of OVA in an alum adjuvant (Fig. 3d). LIPSTIC labelling was observed as early as 24 h after immunization on a small fraction of MHC-II^{hi} dendritic cells, which are likely to be pioneer antigen-presenting cells that drive the initiation of the T cell response in the draining lymph node. The fraction of labelled dendritic cells increased over time, peaking at 10–15% of all dendritic cells at 72 h after immunization (Fig. 3e–f and Extended Data Fig. 7l). Phenotypic analysis showed that labelling was restricted to MHC-II^{hi} dendritic cells, which were mostly CD11b$^+$. Labelling of XCR1$^+$ dendritic cells was a rare event, and was observed consistently—albeit

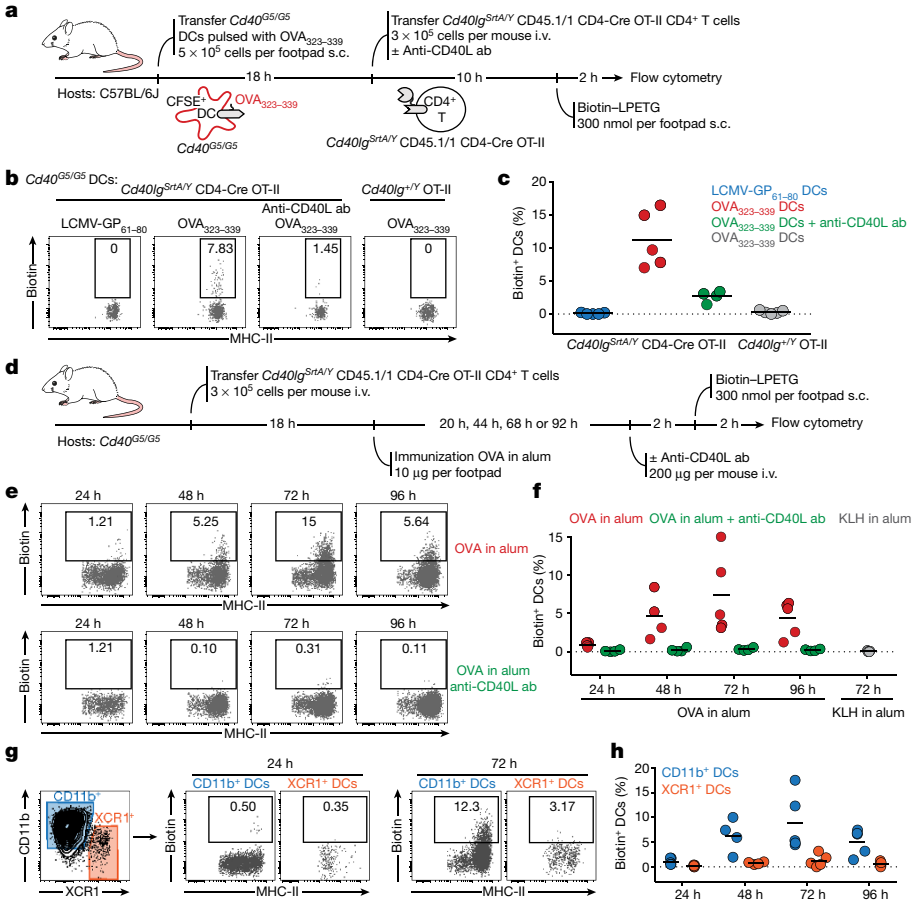

Figure 3 | LIPSTIC enables monitoring of CD40–CD40L interactions between T cells and dendritic cells *in vivo*. **a**, Experimental setup for **b**, **c**. CD45.1 encoded by *Ptprc*^{a}; homozygotes are indicated as CD45.1/1. **b**, Flow cytometric analysis of PLN cells showing biotin labelling of transferred *Cd40*$^{G5/G5}$ dendritic cells. **c**, Percentage of biotin$^+$ dendritic cells among transferred dendritic cell populations gated as in **b**. **d**, Experimental setup for **e**–**h**. **e**, Flow cytometric analysis of PLN cells showing biotin labelling of endogenous dendritic cells at different times after immunization in mice left untreated (top) or treated with a CD40L-blocking antibody (bottom). **f**, Percentage of biotin$^+$ dendritic cells among endogenous dendritic cells gated as in **e**. **g**, Flow cytometric analysis of PLN cells showing biotin labelling among endogenous CD11b$^+$ or XCR1$^+$ dendritic cells at 24 or 72 h after immunization. **h**, Percentage of biotin$^+$ dendritic cells among endogenous CD11b$^+$ or XCR1$^+$ dendritic cells gated as in **g**. **c**, **f**, **h**, Each symbol represents one mouse; bars indicate the mean. Data are pooled from two independent experiments. i.v., intravenous injection; s.c., subcutaneous injection.

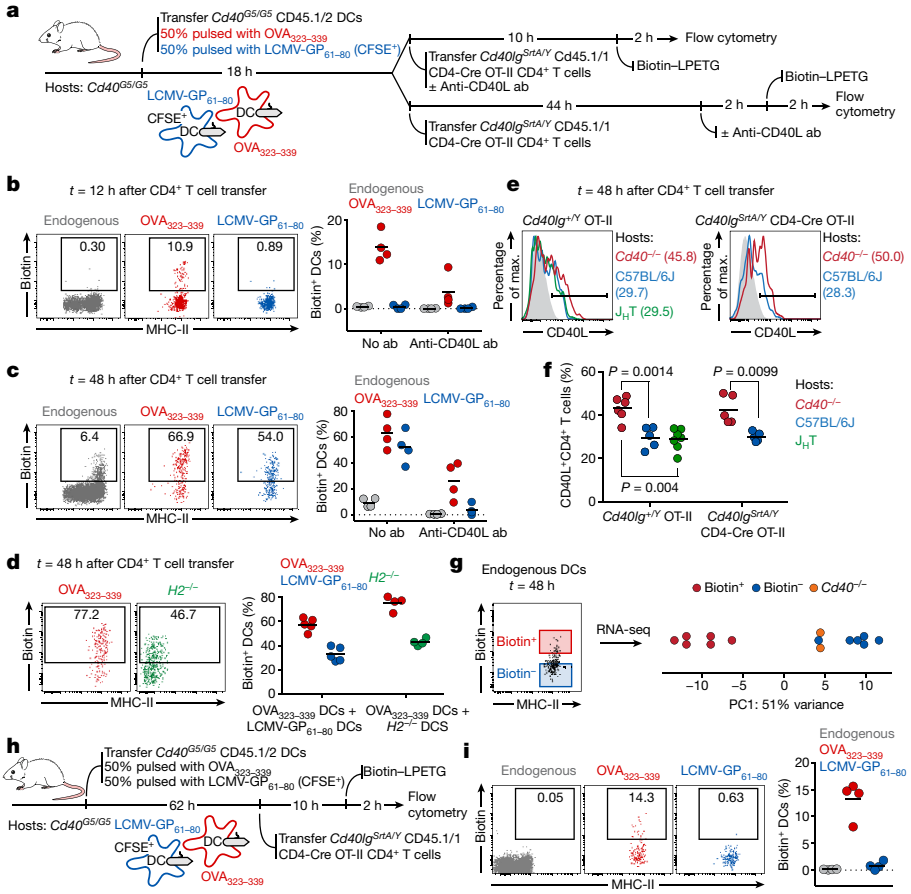

Figure 4 | Different modalities of the CD40–CD40L interaction between CD4$^+$ T cells and dendritic cells *in vivo*. **a**, Experimental setup for **b**, **c**. **b**, **c**, Flow cytometric analysis of PLN cells showing biotin labelling of endogenous and transferred dendritic cells 12 h (**b**) or 48 h (**c**) after T-cell transfer. **d**, Flow cytometry of PLN cells showing biotin labelling of transferred dendritic cells 48 h after T-cell transfer. Experimental setup as in **a**, except that bystander dendritic cells are *H2*$^{-/-}$ cells. **e**, CD40L expression in activated CD4$^+$ T cells. Histograms show CD40L surface staining in *Cd40lg*$^{+/Y}$ OT-II (left) or *Cd40lg*$^{SrtA/Y}$ CD4-Cre OT-II (right) CD69$^+$ CD4$^+$ T cells. Data are representative of two independent experiments. **f**, Percentage of CD69$^+$ CD4$^+$ T cells positive for CD40L. One-way ANOVA with Tukey's post hoc test and unpaired two-tailed Student's *t*-test were used for statistical analysis. **g**, Principal component analysis of transcriptomic profiles of endogenous biotin$^+$ and biotin$^-$ MHC-II^{hi}CD11c$^+$CD11b$^+$XCR1$^-$ dendritic cells sorted 48 h after T-cell transfer from mice treated as in **a**. Each symbol represents one sample derived from one mouse in a single experiment. **h**, Experimental setup for **i**. CD45.1 encoded by Ptprc^a; homozygotes are indicated as CD45.1/1. CD45.2 is encoded by Ptprc^b. Heterozygotes are indicated as CD45.1/2. **i**, Left, flow cytometry of PLN cells showing biotin labelling of endogenous and transferred *Cd40*$^{G5/G5}$ dendritic cells 12 h after T-cell transfer. Right, percentage of biotin$^+$ dendritic cells gated as shown among different dendritic cell populations. **b**–**d**, **f**, **i**, Each symbol represents one mouse; bars indicate the mean; data are pooled from two independent experiments.

at low levels—only at 72 h after immunization, in line with previous reports that used intravital imaging and histocytometry[12] (Fig. 3g, h). We conclude that LIPSTIC can be used to follow the dynamics of CD40–CD40L contacts between T cells and dendritic cells *in vivo*, with a sufficient signal-to-noise ratio to detect rare and low-intensity interactions.

The finding that the CD40–CD40L interaction between T cells and dendritic cells peaks at 72 h after immunization (Fig. 3f), in addition to previous studies that have suggested that CD40L may, under certain circumstances, engage its receptor in the absence of antigen presentation[13–15], led us to hypothesize that LIPSTIC labelling later in the response may reflect non-cognate interactions between T cells and dendritic cells taking place during the motile 'phase 3' of T-cell priming[10]. To test this hypothesis, we co-transferred into *Cd40*$^{G5/G5}$ hosts two populations of dendritic cells treated independently with either OVA$_{323–339}$ (the cognate population) or LCMV-GP$_{61–80}$ (the bystander population), followed by OT-II–SrtA CD4$^+$ T cells (Fig. 4a). Whereas LIPSTIC labelling at 12 h after T-cell transfer was detected only on cognate dendritic cells, specificity was lost at 48 h, when both transferred and endogenous bystander dendritic cells were robustly labelled (Fig. 4b, c and Extended Data Fig. 8a). To verify that bystander labelling was truly non-cognate—as opposed to resulting from transfer of antigenic peptide between dendritic cell populations—we performed identical co-transfer experiments, but using *H2*$^{-/-}$ dendritic cells as bystanders. LIPSTIC labelling of *H2*$^{-/-}$ dendritic cells at late time points was indistinguishable from that of MHC-II-sufficient bystanders under the same conditions (Fig. 4d). Non-cognate LIPSTIC labelling of bystander dendritic cells at later time points was also observed after OVA immunization of haematopoietic chimaeras reconstituted with 80% *Cd40*$^{G5/G5}$ and 20% *Cd40*$^{G5/G5}$;*H2*$^{-/-}$ bone marrow (Extended Data Fig. 8c–e), and during *ex vivo* priming experiments analogous to those described in Fig. 2 (Extended Data Fig. 9). Thus, CD40L–CD40 LIPSTIC labelling during late stages of T-cell priming is not restricted to dendritic cells presenting the cognate antigen, in three distinct priming models.

To confirm non-cognate CD40–CD40L interactions in a system independent of LIPSTIC, we took advantage of the observation that CD40-dependent downregulation of surface CD40L on T cells can be used as a surrogate reporter for the CD40–CD40L interaction *in vivo*[14]. We injected wild-type OVA$_{323–339}$-treated dendritic cells into either wild-type or *Cd40*$^{-/-}$ hosts, transferred OT-II CD4$^+$ T cells one day later, then analysed CD40L expression at 48 h after

T-cell transfer. Whereas downregulation of CD40L could be observed in T cells transferred into wild-type hosts, this was not the case for T cells transferred into *Cd40*$^{-/-}$ hosts, despite the presence of CD40 on the transferred Ag-loaded dendritic cells. CD40L downregulation was comparable in wild-type and in B-cell-deficient (J_HT) hosts, indicating that B cells do not contribute to CD40L downregulation (Fig. 4e, f). Thus, CD40L–CD40 interactions between T cells and with non-B cell antigen-presenting cells that are not loaded with antigen can downregulate surface CD40L on the T cell, confirming the interactions between activated T cells and bystander dendritic cells revealed by LIPTSIC. Moreover, similar downregulation of CD40L was observed in OT-II–SrtA T cells, indicating that the SrtA fusion does not prevent the downregulation of CD40L after it engages CD40 (Fig. 4e–f).

Gene expression profiling of bystander biotin$^+$ and biotin$^-$ host dendritic cells revealed clear differences between these two populations. Principal component analysis detected a major component (accounting for 51% of total variance) for which biotin$^+$ dendritic cells were clearly separated from biotin$^-$ dendritic cells, which in turn resembled bystander dendritic cells from mice lacking CD40 (Fig. 4g), a conclusion also supported by hierarchical clustering (Extended Data Fig. 10c). Differential expression analysis identified 788 genes that differed significantly between conditions (fold change >2 and false-discovery rate <0.05) (listed in Extended Data Fig. 10d and Supplementary Table1). We conclude that bystander interactions between T cells and dendritic cells are associated with marked changes in gene expression, and CD40 ligation potentially has a role in these alterations.

Finally, to determine whether the change in the pattern of interaction between T cells and dendritic cells over time is due to a change in the properties of T cells or of dendritic cells, we repeated the $OVA_{323–339}$/LCMV-$GP_{61–80}$ dendritic cell co-transfer experiment but this time delaying T-cell transfer to 62 h after dendritic cell injection, so that, at the time of labelling, dendritic cells had been in the host for 70 h but T cells for only 12 h (Fig. 4h). This rescued the specificity of T-cell interactions, in that only dendritic cells treated with $OVA_{323–339}$ peptide were labelled (Fig. 4i). Thus, newly primed T cells retain their specificity even when antigen-bearing dendritic cells have been present for several days. We conclude that CD40-CD40L interactions between CD4$^+$ T cells and dendritic cells proceed in two stages. Initially, CD40L signals from arrested T cells are delivered specifically to antigen-loaded dendritic cells that are priming the response. This is followed by an antigen-independent stage in which motile, activated T cells are capable of interacting via CD40L even with dendritic cells that are not presenting the cognate antigen.

We introduce LIPSTIC, a novel system for labelling cell–cell interactions enzymatically both *in vitro* and *in vivo*. Although similar approaches have been proposed previously[16–18], our system has a number of unique features: first, the use of a mutated version of SrtA with low affinity for the N-terminal oligoglycine makes SrtA less likely to be the driver of the cell–cell interaction and more likely to operate as a readout of interactions driven by high-affinity receptor–ligand pairs. Second, SrtA uses a peptide substrate that is easily synthesized and can be linked to a wide variety of detectable labels, including genetically encoded fluorescent proteins or epitope tags[2]. Third, and most importantly, SrtA substrates can be readily administered to live animals, allowing us to detect and isolate cells based on their history of intercellular interactions *in vivo*. Given the importance of such interactions to immunology and other fields of biomedical science, we expect this technology will be widely useful to biologists in general, representing a useful complement to intravital microscopy.

Online Content Methods, along with any additional Extended Data display items and Source Data, are available in the online version of the paper; references unique to these sections appear only in the online paper.

Received 14 June; accepted 8 December 2017.
Published online 17 January 2018.

1. Cahalan, M. D. & Parker, I. Choreography of cell motility and interaction dynamics imaged by two-photon microscopy in lymphoid organs. *Annu. Rev. Immunol.* **26,** 585–626 (2008).
2. Popp, M. W. & Ploegh, H. L. Making and breaking peptide bonds: protein engineering using sortase. *Angew. Chem. Int. Ed. Engl.* **50,** 5024–5032 (2011).
3. Chen, I., Dorr, B. M. & Liu, D. R. A general strategy for the evolution of bond-forming enzymes using yeast display. *Proc. Natl Acad. Sci. USA* **108,** 11399–11404 (2011).
4. Haswell, L. E., Glennie, M. J. & Al-Shamkhani, A. Analysis of the oligomeric requirement for signaling by CD40 using soluble multimeric forms of its ligand, CD154. *Eur. J. Immunol.* **31,** 3094–3100 (2001).
5. Ghiotto, M. *et al.* PD-L1 and PD-L2 differ in their molecular mechanisms of interaction with PD-1. *Int. Immunol.* **22,** 651–660 (2010).
6. van der Merwe, P. A., Bodian, D. L., Daenke, S., Linsley, P. & Davis, S. J. CD80 (B7-1) binds both CD28 and CTLA-4 with a low affinity and very fast kinetics. *J. Exp. Med.* **185,** 393–404 (1997).
7. Greene, J. L. *et al.* Covalent dimerization of CD28/CTLA-4 and oligomerization of CD80/CD86 regulate T cell costimulatory interactions. *J. Biol. Chem.* **271,** 26762–26771 (1996).
8. An, H.-J. *et al.* Crystallographic and mutational analysis of the CD40–CD154 complex and its implications for receptor activation. *J. Biol. Chem.* **286,** 11226–11235 (2011).
9. Singh, J. *et al.* The role of polar interactions in the molecular recognition of CD40L with its receptor CD40. *Protein Sci.* **7,** 1124–1135 (1998).
10. Mempel, T. R., Henrickson, S. E. & Von Andrian, U. H. T-cell priming by dendritic cells in lymph nodes occurs in three distinct phases. *Nature* **427,** 154–159 (2004).
11. Swee, L. K., Lourido, S., Bell, G. W., Ingram, J. R. & Ploegh, H. L. One-step enzymatic modification of the cell surface redirects cellular cytotoxicity and parasite tropism. *ACS Chem. Biol.* **10,** 460–465 (2015).
12. Eickhoff, S. *et al.* Robust anti-viral immunity requires multiple distinct T cell–dendritic cell interactions. *Cell* **162,** 1322–1337 (2015).
13. Kretschmer, B., Kühl, S., Fleischer, B. & Breloer, M. Activated T cells induce rapid CD83 expression on B cells by engagement of CD40. *Immunol. Lett.* **136,** 221–227 (2011).
14. Lesley, R., Kelly, L. M., Xu, Y. & Cyster, J. G. Naive CD4 T cells constitutively express CD40L and augment autoreactive B cell survival. *Proc. Natl Acad. Sci. USA* **103,** 10717–10722 (2006).
15. Behrens, G. M. *et al.* Helper requirements for generation of effector CTL to islet β cell antigens. *J. Immunol.* **172,** 5420–5426 (2004).
16. Liu, D. S., Loh, K. H., Lam, S. S., White, K. A. & Ting, A. Y. Imaging trans-cellular neurexin–neuroligin interactions by enzymatic probe ligation. *PLoS ONE* **8,** e52823 (2013).
17. Slavoff, S. A., Liu, D. S., Cohen, J. D. & Ting, A. Y. Imaging protein–protein interactions inside living cells via interaction-dependent fluorophore ligation. *J. Am. Chem. Soc.* **133,** 19769–19776 (2011).
18. Martell, J. D. *et al.* A split horseradish peroxidase for the detection of intercellular protein–protein interactions and sensitive visualization of synapses. *Nat. Biotechnol.* **34,** 774–780 (2016).

Supplementary Information is available in the online version of the paper.

Acknowledgements We thank H. Ploegh for introducing us to sortase A; H. Yang, S. Markoulaki and R. Jaenisch for generating gene-targeted mice; A. Ting for NLG- and NRX-expressing constructs; and L. Mesin and C. F. Opel for technical advice. This work was funded by NIH grants DP5OD012146 and R01AI119006 to G.D.V. and a Starr Cancer Consortium grant to G.D.V. and N.H. G.P. was supported by the Swiss National Science Foundation Postdoctoral fellowship and the Cancer Research Institute Irvington Postdoctoral fellowship. G.V. is a Searle Scholar.

Author Contributions G.P. and G.D.V. conceived the study, designed and analysed experiments and wrote the manuscript. G.P. performed all experimental work (with the exception of gene-expression analysis), with sporadic assistance from A.Ch., J.M.T. and M.A. L.D.S., A.Cu. and N.H. contributed the gene-expression profiling work, including experiments and data analysis presented in Fig. 4g and Extended Data Fig. 10 and wrote the text for these experiments.

Author Information Reprints and permissions information is available at www.nature.com/reprints. The authors declare competing financial interests: details are available in the online version of the paper. Readers are welcome to comment on the online version of the paper. Publisher's note: Springer Nature remains neutral with regard to jurisdictional claims in published maps and institutional affiliations. Correspondence and requests for materials should be addressed to G.D.V. (victora@rockefeller.edu).

Reviewer Information *Nature* thanks M. Dustin, A. Esser-Kahn, T. Mempel and the other anonymous reviewer(s) for their contribution to the peer review of this work.

METHODS

Data reporting. No statistical methods were used to predetermine sample size. The experiments were not randomized and the investigators were not blinded to allocation during experiments and outcome assessment.

Plasmids. All constructs were cloned into the pMP71 vector[19], which was modified to express a fluorescent reporter (eGFP or Tomato) followed by the porcine teschovirus-1 self-cleavable 2A peptide[20] and the protein of interest. The SrtA sequence, including a terminal Flag-tag, was attached by a double 218 linker[21] to the extracellular terminus of the modified receptor or ligand (C or N terminus, depending on protein topology). A five-glycine tag (G5) followed by a Myc tag was fused at the N terminus of modified receptors or ligands. The sequences of all constructs used are included in Supplementary Table 2.

Mice. C57BL6/J, CD45.1 (B6.SJL *Ptprc*^{a}), *Cd40*$^{-/-}$ (ref. 22), *Cd40lg*$^{-/-}$ (ref. 23), *H2*$^{-/-}$ (ref. 24), CD4-Cre-transgenic[25] and eCFP-transgenic[26] mice were purchased from The Jackson Laboratory (strain numbers 000664, 002014, 002928, 002770, 003584, 022071 and 004218, respectively). *Cd40*^{G5} and *Cd40lg*^{SrtA} mice were generated and maintained in our laboratories. B1-8^{hi} (ref. 27), J_HT (ref. 28) and OT-II TCR transgenic (Y chromosome)[29] mice were originally provided by M. Nussenzweig (Rockefeller University). All mice were housed in specific pathogen-free facilities at the Whitehead Institute for Biomedical Research and The Rockefeller University in accordance with institutional guidelines and ethical regulations. All protocols were approved by the Massachusetts Institute of Technology Committee for Animal Care and the Rockefeller University Institutional Animal Care and Use Committee. Male and female 5–12-week-old mice were used in all experiments.

Generation of *Cd40*^{G5} and *Cd40lg*^{SrtA} mice. The *Cd40*^{G5} mouse line was generated using CRISPR–Cas9 gene targeting by cytoplasmic injection of *Cas9* mRNA, chimeric single-guide RNA (sgRNA) and a repair oligonucleotide into fertilized C57BL/6 zygotes at the one-cell stage, as previously described[30,31].

The sequence for the dsDNA template for chimeric *Cd40*^{G5} sgRNA transcription was as follows (protospacer sequence is underlined): CGCTGTTAATACGACTCACTATAGGTCTGTTTTTAGGTCCATCTAGTTTTAGAGCTAGAAATAGCAAGTTAAAATAAGGCTAGTCCGTTATCAACTTGAAAAAGTGGCACCGAGTCGGTGCTTTT.

The *Cd40*^{G5} repair oligonucleotide was synthesized as an ssDNA ultramer and PAGE-purified (Integrated DNA Technologies). The repair oligonucleotide sequence was as follows (differences from the wild-type C57BL/6 sequence are underlined): TGGCTGGCACAAATCACAGCACTGGCCATCGTGGAGGTACTGTTTGTCACTGCACGTAACGGTACCTCCTCCGCCTCCACACTGCCCTAGATGTACCTAAAAACAGAAGTGGACAGCTGGAAGGGATCTTCCACCGGC.

The *Cd40lg*^{SrtA} mouse line was generated using CRISPR–Cas9 gene targeting by cytoplasmic injection of *Cas9* mRNA, chimeric sgRNA, SCR7 (an NHEJ inhibitor, Excess Bioscience) and the repair plasmid into fertilized C57BL/6 zygotes at the one-cell stage, as described in ref. 32, with the exception that the final concentration of SCR7 used was 100 μM.

The sequence of the dsDNA template for chimeric *Cd40lg*^{SrtA} sgRNA transcription was as follows (protospacer sequence is underlined): CGCTGTTAATACGACTCACTATAGGAGTTGGCTTCTCATCTTTGTTTTAGAGCTAGAAATAGCAAGTTAAAATAAGGCTAGTCCGTTATCAACTTGAAAAAGTGGCACCGAGTCGGTGCTTTT.

The sequence of the *Cd40lg*^{SrtA} targeting construct is reported in Supplementary Table 2.

Cas9 mRNA was purchased from Sigma-Aldrich. Chimeric sgRNAs were *in vitro*-transcribed from a synthetic dsDNA template (gBlocks, Integrated DNA Technologies) using the MEGAshortscript T7 Transcription Kit (Thermo Fisher Scientific) and purified using Ampure XP beads (Beckman Coulter).

Isolation of splenic dendritic cells, CD4$^+$ T cells and B cells. To isolate dendritic cells, spleens were collected, incubated for 30 min at 37 °C in RPMI, 2% FBS, 20 mM HEPES, 400 U ml^{-1} type-IV collagenase (Worthington Biochemical) and disrupted to generate single-cell suspensions. Red-blood cells were lysed with ACK buffer (Lonza), and the resulting cell suspensions were filtered through a 70-μm mesh into PBS supplemented with 0.5% BSA and 2 mM EDTA (PBE). Dendritic cells were obtained by magnetic cell separation (MACS) using anti-CD11c beads (Miltenyi Biotec), as per the manufacturer's instructions. To isolate CD4$^+$ T cells and B cells, spleens were processed as above, except for collagenase digestion, which was not performed. CD4$^+$ T cells were isolated using the CD4$^+$ T cell isolation kit (Miltenyi Biotec), whereas B cells were obtained by negative selection using anti-CD43 beads (Miltenyi Biotec), as per the manufacturer's instructions. To isolate Igλ$^+$ B cells from B1-8^{hi} mice, B cells were stained with anti-Igκ-PE antibody and subsequently purified by negative selection using a combination of anti-CD43 and anti-PE magnetic beads (Miltenyi Biotec).

Cell transfers, immunizations and treatments. For dendritic cell transfer experiments, splenic dendritic cells isolated as described above were resuspended at 10^7 cells per ml and treated with 10 μM $OVA_{323–339}$ or LCMV-$GP_{61–80}$ (both from Anaspec) in RPMI, 10% FBS, for 30 min at 37 °C. For cell labelling, CFSE was added to a final concentration of 2 μM during the last 5 min of incubation. Cells were then washed three times in RPMI, 10% FBS and resuspended at 2×10^7 cells per ml in PBS supplemented with 0.4 μg ml^{-1} LPS. Dendritic cells were injected (5×10^5 cells in 25 μl) by subcutaneous injection into the hind footpad. For CD4$^+$ T-cell transfer experiments, CD4$^+$ T cells isolated as described above were resuspended at 3×10^6 cells per ml in PBS and injected intravenously (3×10^5 cells in 100 μl per mouse).

For immunization experiments, mice were immunized by subcutaneous injection into the hind footpad with 10 μg OVA adsorbed in alum (Imject Alum, Thermo Fisher Scientific) at 2:1 antigen:alum (v:v) ratio in 25 μl volume.

For LIPSTIC *in vivo* labelling experiments, biotin–LPETG (see below) was injected subcutaneously into the hind footpad (20 μl of 2.5 mM solution in PBS, equivalent to 50 nmol). Mice were injected six times 20 min apart, and popliteal lymph nodes were collected 40 min after the last injection. Mice were briefly anaesthetized with isoflurane at each injection.

For CD40L-blockade experiments *in vivo*, mice were injected intravenously with 200 μg of CD40L-blocking antibody (clone MR-1, BioXCell) at the indicated times.

Analysis of CD40L expression *in vivo*. C57BL/6J dendritic cells were treated *ex vivo* with $OVA_{323–339}$ and transferred subcutaneously (5×10^5 per footpad) to *Cd40*$^{-/-}$, C57BL/6J or J_HT hosts. Eighteen hours later, 3×10^5 *Cd40lg*$^{+/Y}$ OT-II or *CD40lg*$^{SrtA/Y}$ CD4-Cre OT-II CD4$^+$ T cells were transferred intravenously and PLN were analysed 48 h after T-cell transfer.

Flow cytometry and cell sorting. Popliteal lymph nodes were collected, incubated for 30 min at 37 °C in RPMI, 2% FBS, 20 mM HEPES, 400 U ml^{-1} type-IV collagenase (Worthington Biochemical), disrupted using disposable micropestles (Axygen) and filtered through a 70-μm cell strainer. Single-cell suspensions were washed with PBE, incubated at room temperature for 5 min with 1 μg ml^{-1} of anti-CD16/32 (2.4G2, BioXCell) and then stained for cell surface markers at 4 °C for 15 min in PBE using the reagents listed in Supplementary Table 3. Cells were washed with PBS and stained with Zombie fixable viability dyes (Biolegend) at room temperature for 15 min and then fixed with Cytofix (BD Biosciences) before acquisition. In all *in vivo* experiments involving detection of biotin–LPETG SrtA substrate, an anti-biotin–PE antibody (Miltenyi Biotec) was exclusively used owing to its lower background compared to streptavidin conjugates. To eliminate unspecific signals derived from PE binding by a fraction of the B-cell population and thus reduce background, PE–Cy7 isotype control-positive cells were excluded from analysis. In all *in vivo* experiments involving detection of CD40L, a biotinylated anti-CD40L antibody (eBioscience) followed by an anti-biotin PE antibody (Miltenyi Biotec) was used. Samples were acquired on Fortessa or LSR-II flow cytometers (BD Biosciences) and data were analysed using FlowJo v.10.0.8 software.

RNA-sequencing of sorted dendritic cell populations. For the dendritic cell sorting experiment, *Cd40*$^{G5/G5}$ dendritic cells were treated with $OVA_{323–339}$ and transferred subcutaneously (5×10^5 per footpad) into *Cd40*$^{G5/G5}$ recipients. Eighteen hours later, 3×10^5 *CD40lg*$^{SrtA/Y}$ CD4-Cre OT-II CD4$^+$ T cells were transferred intravenously. Biotin–LPETG was administered subcutaneously (300 nmol per footpad) 46 h after T-cell transfer. Popliteal lymph nodes were processed 48 h after T-cell transfer and stained for surface markers as above and endogenous biotin$^+$ and biotin$^-$MHC-II^{hi}CD11c$^+$CD11b$^+$XCR1$^-$ dendritic cells were sorted. As controls, MHC-II^{hi}CD11c$^+$CD11b$^+$XCR1$^-$ dendritic cells were also sorted from *Cd40*$^{-/-}$ mice treated as above, except that they received wild-type (instead of *Cd40*$^{G5/G5}$) dendritic cells and wild-type OT-II (instead of *CD40lg*$^{SrtA/Y}$ CD4-Cre OT-II) CD4$^+$ T cells. Fresh cells were sorted (150 cells per sample) directly into plates containing TCL buffer (Qiagen) supplemented with 1% β-mercaptoethanol using a FACS Aria II (BD Biosciences). RNA from sorted populations was isolated using Agencourt RNAClean XP beads (Beckman Coulter). Full-length cDNA and sequencing libraries were prepared using the Smart-seq2 protocol as previously described[33]. Libraries were sequenced on a Nextseq500 (Illumina) to generate 38-base-pair, paired-end reads.

Raw sequencing data were processed as described[34]. In brief, short sequencing reads were aligned to the UCSC mm10 transcriptome using Bowtie2 (v.2.1.0)[35]. These alignments were used as input in RSEM (v.1.2.8)[36] to quantify gene expression levels for all UCSC mm10 genes in all samples. Data were normalized and analysed using the R software package DESeq2 (v.1.16.0)[37]. Genes with low read counts, defined as those that do not have a normalized expression value greater than 100 in at least three samples, were filtered out, leaving 10,196 genes for the downstream analysis. The 500 genes with the largest variance were used for the principal component analysis and hierarchical clustering. For hierarchical clustering, the complete linkage clustering method was applied on pairwise

distances, defined as 1 minus the Pearson correlation coefficient. Paired differential expression analysis was performed for comparison between biotin$^+$ and biotin$^-$ dendritic cell samples. The differentially expressed genes were compared against the MSigDB database to compute for enrichment using the hypergeometric test[38].

Bone marrow chimaeras. C57BL6/J recipient mice were lethally irradiated with two doses of 450 Rads given 4 h apart. After irradiation, recipients were reconstituted by intravenous injection of haematopoietic cells collected from femurs and tibiae of donor mice. Mice were used for experiments 8–12 weeks after irradiation.

Western blot. Cells were lysed in sample buffer supplemented with 100 mM dithiothreitol. Cell lysates were heated at 98 °C for 5 min and then cleared by centrifugation at 15,000*g* for 10 min. Samples were separated by SDS–PAGE and transferred onto a nitrocellulose membrane. After blocking in 3% skim milk in PBS, membranes were incubated with 1–10 μg ml^{-1} primary antibody in 3% skim milk in PBS overnight at 4 °C. After several washes in PBS and 0.1% Tween-20 (PBST), secondary antibodies coupled to HRP were applied in PBST for 1 h at room temperature when necessary. Blots were developed using Western Lightning ECL (Perkin-Elmer) and BioMax MR films (Kodak).

SrtA substrates. Biotin–aminohexanoic acid–LPETGS (C-terminal amide, 95% purity) was purchased from LifeTein (custom synthesis) and stock solutions prepared in PBS at 20 mM.

SELPETGG (C-terminal amide, 95% purity) was purchased from LifeTein (custom synthesis) and conjugated with AlexaFluor647 succinimidyl ester dye (Thermo Fisher Scientific). Reacted peptides were purified by HPLC.

Southern blot. Genomic DNA (10 μg) purified from mouse tails was digested with XbaI and separated on 0.8% agarose gel. Transfer and hybridization was performed as described[39]. Blots were developed using Storage Phosphor Screens (GE Healthcare) and a Typhoon Imaging System (GE Healthcare). The sequence of the probe used was as follows: GGTCAACCTGGGTTCCATAAAATCTTG TCTTCCCCCAAAAGGGGATAAATTCAGTAGACAGAGGCAGGTAGATCT CTGTGAGTCCCAAGCTAGCCTAGTCTGCATAACAAGTTGTAGGCCAGCT TCTGTTTTCTTTTCTGTCTCAAAAAAGAAAGCAGAAGTGTAAGTGGGT AATGTATTTATTAAACTGAAAAGAATCTGGTCCTTTTTTTCTCATTCAA ATGGTTCAAAAGTGAAAACATCACAAAACAAACATCCTTTATAGAGAA TTTGGGGTGCAATGTATCAG.

LIPSTIC *in vitro*. HEK293T cells (purchased from ATCC) were transfected using the calcium phosphate transfection kit (Thermo Fisher Scientific) with the indicated expression vectors. Forty hours after transfection, cells were detached using a non-enzymatic cell dissociation solution (Thermo Fisher Scientific), washed and resuspended at 10^7 cell per ml in PBS. Cell populations transfected with G5- or SrtA-fusion constructs were mixed at a 1:1 ratio (10^6 cells of each population) in a 1.5-ml conical tube, to which biotin–LPETG was added to a final concentration of 100 μM. Cells were incubated at room temperature for 30 min and washed three times with PBE to remove excess biotin–LPETG before FACS staining or western blot.

Imaging LIPSTIC *in vitro*. B cells and CD4$^+$ T cells were isolated from mouse spleens as described above; B cells were activated with 25 μg ml^{-1} LPS and 10 ng ml^{-1} IL-4, whereas CD4$^+$ T cells were activated with CD3/CD28 dynabeads and rat T-STIM conditioned medium (both from Thermo Fisher Scientific). Twenty-four hours later, cells were transduced with retroviral vectors. Transduced cells were sorted two days after transduction based on expression of the fluorescent reporter present in the retroviral vector. CD4$^+$ T cells were incubated with AlexaFluor647–SELPETGG for 30 min at 37 °C, washed three times, and seeded together with B cells on 8-well Lab-Tek chamber slides (Sigma-Aldrich) previously coated with 12.5 μg ml^{-1} ICAM (2×10^5 cells per well, 1:1 ratio). Cells were immediately imaged using an Andor widefield microscope equipped with a live-cell incubation system. Images were acquired with a 40× objective every 45 s for 90 min using Metamorph software.

LIPSTIC *ex vivo*. Dendritic cells, B cells and CD4$^+$ T cells were isolated from mouse spleens as described above.

Isolated dendritic cells were treated for 2.5 h at 37 °C with the indicated concentration of $OVA_{323–339}$ or LCMV-$GP_{61–80}$ peptides in RPMI, 10% FBS supplemented with LPS (10 μg ml^{-1}), washed three times and then seeded into U-bottom 96-well plates with purified CD4$^+$ T cells (2×10^5 cells per well, 1:1 ratio). Cells were co-cultured for 6 (Fig. 2 and Extended Data Fig. 5) or 24 h (Extended Data Fig. 9), and biotin–LPETG was added at the indicated time of co-culture at a final concentration of 10 μM in complete medium. Blocking antibodies were added at the beginning of co-culture (Fig. 2) or at the indicated times (Extended Data Fig. 9) and used at a final concentration of 150 μg ml^{-1}.

Purified B cells (either polyclonal or Igλ$^+$ B1-8^{hi}) were cooled for 30 min on ice and then incubated for 45 min on ice with the indicated concentrations of NP-OVA (Biosearch Technologies). Cells were then washed twice and seeded into U-bottom 96-well plates with CD4$^+$ T cells (2×10^5 cells per well, 1:1 ratio) previously activated with CD3/CD28 dynabeads (Thermo Fisher Scientific) for 24 h. Cells were co-cultured for 18 h and biotin−LPETG was added during the last 30 min of co-culture at a final concentration of 100 μM in complete medium.

For all experiments, cells were washed three times with PBE before FACS staining to remove excess biotin–LPETG substrate.

Statistical analysis. Statistical tests were conducted using Prism (GraphPad) software. Gaussian distribution was confirmed by the Shapiro–Wilk normality test. Unpaired, two-tailed Student's *t*-tests and one-way ANOVA with Tukey's post hoc tests to further examine pairwise differences were used.

Data availability. RNA-sequencing data are deposited in GEO under accession number GSE107643. All other data are included within the article and the Supplementary Information or are available upon request from the corresponding author.

19. Engels, B. *et al.* Retroviral vectors for high-level transgene expression in T lymphocytes. *Hum. Gene Ther.* **14,** 1155–1168 (2003).
20. Kim, J. H. *et al.* High cleavage efficiency of a 2A peptide derived from porcine teschovirus-1 in human cell lines, zebrafish and mice. *PLoS ONE* **6,** e18556 (2011).
21. Whitlow, M. *et al.* An improved linker for single-chain Fv with reduced aggregation and enhanced proteolytic stability. *Protein Eng.* **6,** 989–995 (1993).
22. Kawabe, T. *et al.* The immune responses in CD40-deficient mice: impaired immunoglobulin class switching and germinal center formation. *Immunity* **1,** 167–178 (1994).
23. Renshaw, B. R. *et al.* Humoral immune responses in CD40 ligand-deficient mice. *J. Exp. Med.* **180,** 1889–1900 (1994).
24. Madsen, L. *et al.* Mice lacking all conventional MHC class II genes. *Proc. Natl Acad. Sci. USA* **96,** 10338–10343 (1999).
25. Lee, P. P. *et al.* A critical role for Dnmt1 and DNA methylation in T cell development, function, and survival. *Immunity* **15,** 763–774 (2001).
26. Hadjantonakis, A. K., Macmaster, S. & Nagy, A. Embryonic stem cells and mice expressing different GFP variants for multiple non-invasive reporter usage within a single animal. *BMC Biotechnol.* **2,** 11 (2002).
27. Shih, T. A., Roederer, M. & Nussenzweig, M. C. Role of antigen receptor affinity in T cell-independent antibody responses *in vivo*. *Nat. Immunol.* **3,** 399–406 (2002).
28. Gu, H., Zou, Y. R. & Rajewsky, K. Independent control of immunoglobulin switch recombination at individual switch regions evidenced through Cre–loxP-mediated gene targeting. *Cell* **73,** 1155–1164 (1993).
29. Barnden, M. J., Allison, J., Heath, W. R. & Carbone, F. R. Defective TCR expression in transgenic mice constructed using cDNA-based α- and β-chain genes under the control of heterologous regulatory elements. *Immunol. Cell Biol.* **76,** 34–40 (1998).
30. Yang, H. *et al.* One-step generation of mice carrying reporter and conditional alleles by CRISPR/Cas-mediated genome engineering. *Cell* **154,** 1370–1379 (2013).
31. Wang, H. *et al.* One-step generation of mice carrying mutations in multiple genes by CRISPR/Cas-mediated genome engineering. *Cell* **153,** 910–918 (2013).
32. Maruyama, T. *et al.* Increasing the efficiency of precise genome editing with CRISPR–Cas9 by inhibition of nonhomologous end joining. *Nat. Biotechnol.* **33,** 538–542 (2015).
33. Picelli, S. *et al.* Full-length RNA-seq from single cells using Smart-seq2. *Nat. Protoc.* **9,** 171–181 (2014).
34. Shalek, A. K. *et al.* Single-cell RNA-seq reveals dynamic paracrine control of cellular variation. *Nature* **510,** 363–369 (2014).
35. Langmead, B. & Salzberg, S. L. Fast gapped-read alignment with Bowtie 2. *Nat. Methods* **9,** 357–359 (2012).
36. Li, B. & Dewey, C. N. RSEM: accurate transcript quantification from RNA-seq data with or without a reference genome. *BMC Bioinformatics* **12,** 323 (2011).
37. Love, M. I., Huber, W. & Anders, S. Moderated estimation of fold change and dispersion for RNA-seq data with DESeq2. *Genome Biol.* **15,** 550 (2014).
38. Subramanian, A. *et al.* Gene set enrichment analysis: a knowledge-based approach for interpreting genome-wide expression profiles. *Proc. Natl Acad. Sci. USA* **102,** 15545–15550 (2005).
39. Southern, E. Southern blotting. *Nat. Protoc.* **1,** 518–525 (2006).

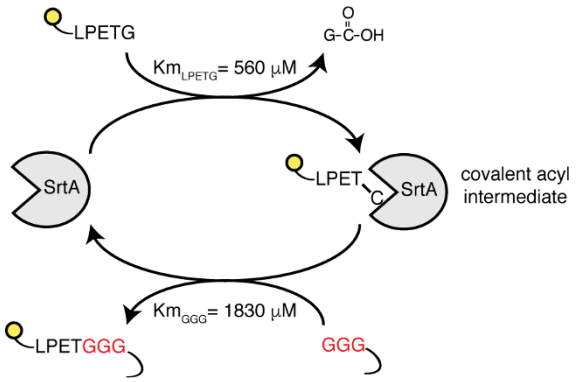

Extended Data Figure 1 | Schematic representation of the SrtA reaction. The SrtA enzyme recognizes the short amino acid sequence LP*X*TG (where *X* is any amino acid). Upon binding, SrtA forms a covalent acyl intermediate between the threonine of the substrate and the cysteine present in its catalytic pocket. The reaction proceeds with the formation of an amide bond between substrate threonine and an N-terminal glycine. Affinities displayed refer to engineered SrtA variants carrying P94S, D160N, and K196T mutations.

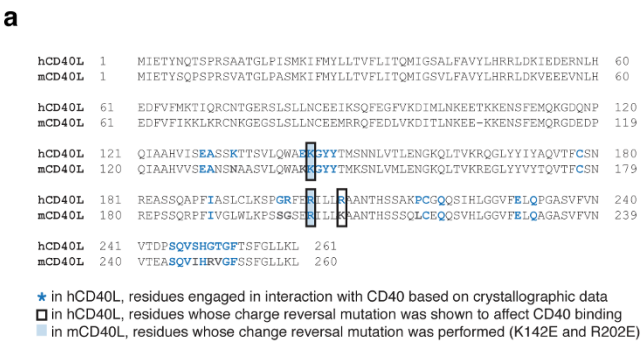

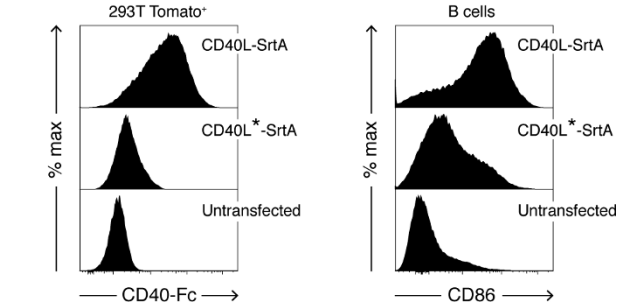

Extended Data Figure 2 | Two point mutations in the mouse CD40L coding sequence impair binding to CD40. a, Sequence alignment of human and mouse CD40L proteins. Owing to the lack of crystallographic data describing the mouse CD40–CD40L complex, we identified residues potentially engaged in CD40 binding on the basis of information available for the human CD40–CD40L complex. Residues in human CD40L sequences engaged in the interaction with CD40 based on crystallographic data are highlighted in blue. Among these, residues for which a charge reversal mutation was shown to affect CD40 binding are boxed. Filled boxes identify the residues in mouse CD40L for which a charge reversal mutation was performed (K142E and R202E). Mutations at equivalent locations in the human CD40L coding sequence (K143, R203) have also been detected in patients with hyper-IgM syndrome. CD40L with both mutations (K142E and R202E) is labelled as CD40L*. **b**, Binding of CD40 to CD40L–SrtA and CD40L*–SrtA. HEK293T cells were transfected with CD40L–SrtA or CD40L*–SrtA, incubated with CD40–Fc protein and analysed by flow cytometry. Histograms show severe impairment of CD40 binding to CD40L*–SrtA. **c**, B-cell activation by CD40L–SrtA and CD40L*–SrtA. Primary mouse B cells were cultured on a monolayer of HEK293T cells expressing CD40L–SrtA or CD40L*–SrtA. CD86 surface expression was analysed by flow cytometry 18 h later. Histograms show reduced upregulation of CD86 in B cells stimulated with CD40L*–SrtA. Data are representative of two independent experiments.

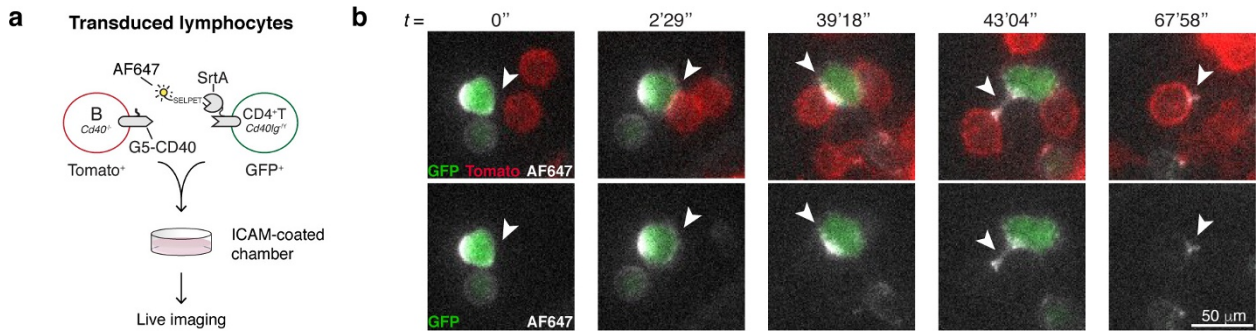

Extended Data Figure 3 | Imaging of LIPSTIC labelling. a, Experimental setup for live imaging of LIPSTIC labelling. *Cd40*$^{-/-}$ B cells and *Cd40lg*$^{-/Y}$ CD4^{+} T cells were transduced with G5–CD40 (Tomato reporter) or CD40L–SrtA (GFP reporter), respectively. CD40L–SrtA^{+} T cells were loaded with AlexaFluor647–SELPETGG, mixed with G5–CD40^{+} B cells on intercellular adhesion molecule (ICAM)-coated chambers to allow interactions and were immediately imaged. **b**, Time-series showing transfer of AlexaFluor647–SELPETGG (white) from CD40L–SrtA^{+} T cells (green) to G5–CD40^{+} B cells (red) upon interaction. Data are representative of two independent experiments.

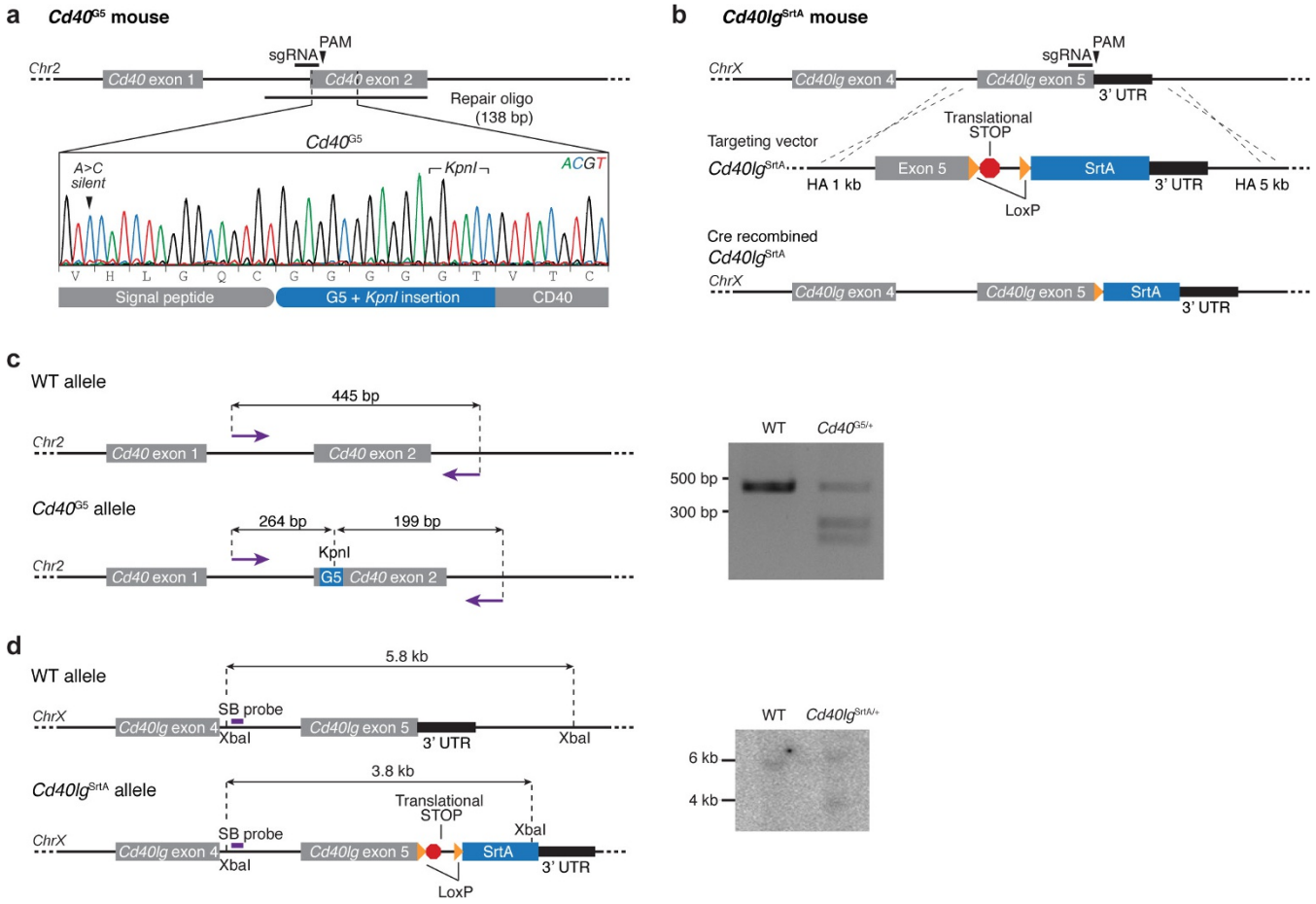

Extended Data Figure 4 | Generation of *Cd40*^{G5} and *Cd40lg*^{SrtA} gene-targeted mice. a, **b**, Schematic representation and CRISPR–Cas9 genome-editing strategy for the *Cd40*^{G5} (**a**) and *Cd40lg*^{SrtA} (**b**) alleles. HA, homology arm; PAM, protospacer adjacent motif. **c**, Restriction fragment length polymorphism analysis of *Cd40*$^{G5/+}$ mice. PCR products generated using primers surrounding the G5 insertion site were digested with KpnI and analysed by electrophoresis on an agarose gel. WT, wild type. Data are representative of at least two experiments. **d**, Southern blot analysis of a *Cd40lg*$^{SrtA/+}$ mouse. Genomic DNA was extracted, digested with XbaI, and transferred onto a nitrocellulose membrane after electrophoresis on an agarose gel. Genomic DNA fragments were detected using a probe annealing between exons 4 and 5.

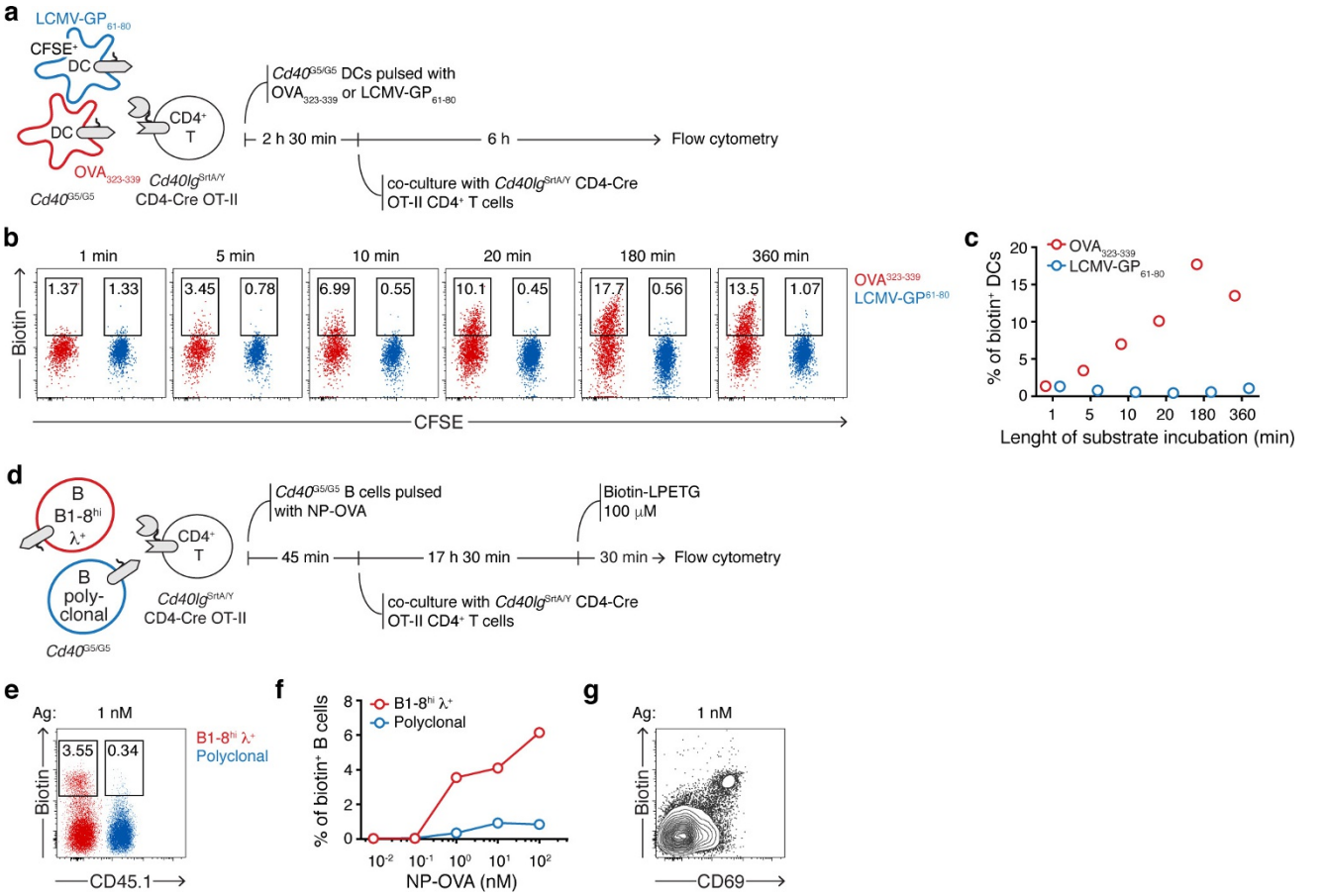

Extended Data Figure 5 | LIPSTIC labelling *ex vivo*. a, Experimental setup used in **b**, **c** to assess the influence of substrate incubation length on intercellular labelling between primary dendritic cells and $CD4^+$ T cells. $Cd40^{G5/G5}$ dendritic cells populations were separately treated with 1 μM of $OVA_{323–339}$ or LCMV-$GP_{61–80}$, mixed and co-cultured for 6 h with $Cd40lg^{SrtA/Y}$ CD4-Cre OT-II $CD4^+$ T cells. Biotin–LPETG was added during the final 1, 5, 10, 20, 180 min of co-culture or for the entire co-culture time (360 min) at a final concentration of 10 μM, and cells were analysed by flow cytometry. **b**, Flow cytometric analysis of co-cultured dendritic cells incubated with biotin–LPETG for the indicated times. **c**, Percentage of $biotin^+$ dendritic cells gated as in **b**. **d**, Experimental setup used in **e**–**g** to analyse intercellular labelling *ex vivo* between primary B cells and $CD4^+$ T cells. Two populations of $Cd40^{G5/G5}$ B cells that either carried a wild-type polyclonal B-cell receptor repertoire or expressed the B1-8^{hi} Ig heavy chain, which when paired to an Igλ light chain confers specificity towards the hapten 4-hydroxy-3-nitrophenylacetyl (NP), were mixed and treated with the indicated concentrations of NP-OVA. Cells were then co-cultured for 18 h with $Cd40lg^{SrtA/Y}$ CD4-Cre OT-II $CD4^+$ T cells. Biotin–LPETG was added during the last 30 min of co-culture at a final concentration of 100 μM, and cells analysed by flow cytometry. **e**, Flow cytometric analysis of B cells treated with 1 nM of NP-OVA showing preferential biotin labelling of B1-$8^{hi}\lambda^+$ B cells. **f**, Percentage of $biotin^+$ B cells among polyclonal and B1-$8^{hi}\lambda^+$ populations at the indicated NP-OVA concentrations. **g**, Flow cytometric analysis of B cells treated with 1 nM of NP-OVA showing positive correlation between biotin labelling and expression of the activation marker CD69. Data are representative of three independent experiments.

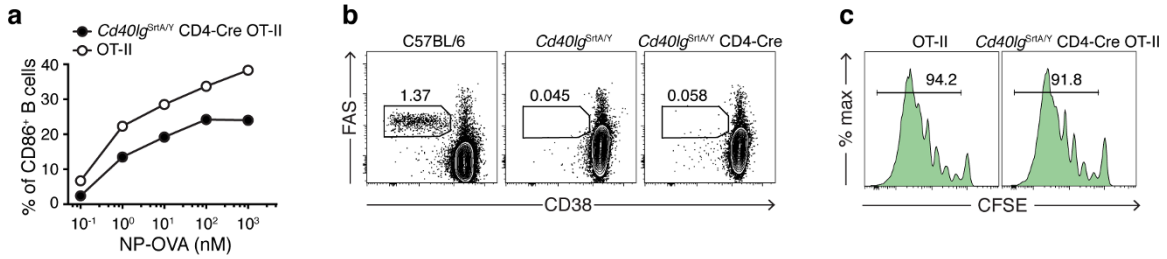

Extended Data Figure 6 | Characterization of *Cd40lg*$^{SrtA/Y}$ T cells. **a**, Upregulation of CD86 on B cells by CD40L–SrtA. B1-8^{hi} λ^+ B cells were treated with the indicated concentrations of NP-OVA and co-cultured with *Cd40lg*$^{SrtA/Y}$ CD4-Cre OT-II or wild-type OT-II CD4$^+$ T cells for 18 h. Cells were analysed by flow cytometry. The percentage of CD86$^+$ B cells when co-cultured with *Cd40lg*$^{SrtA/Y}$ CD4-Cre OT-II or wild-type OT-II T cells in the presence of indicated concentrations of NP-OVA is shown. **b**, Germinal centre formation in *Cd40lg*$^{SrtA/Y}$ and *Cd40lg*$^{SrtA/Y}$ CD4-Cre mice. C57BL/6J, *Cd40lg*$^{+/Y}$ and *Cd40lg*$^{SrtA/Y}$ CD4-Cre mice were immunized subcutaneously with 20 μg of NP-OVA in alum at the base of the tail. Inguinal lymph nodes were analysed by flow cytometry 12 days after immunization. Dot plots show the absence of germinal centre formation in both *Cd40lg*$^{SrtA/Y}$ and *Cd40lg*$^{SrtA/Y}$ CD4-Cre mice, suggestive of an impaired ability of *Cd40lg*$^{SrtA/Y}$ T cells to activate B cells. A similar phenotype is observed regardless of the presence of Cre recombination, which is likely because of the addition of a translated LoxP site to the C terminus of the CD40L protein. **c**, *In vivo* expansion of *Cd40lg*$^{SrtA/Y}$ CD4-Cre OT-II CD4$^+$ T cells. 5×10^5 *Cd40*$^{G5/G5}$ dendritic cells treated *ex vivo* with OVA$_{323–339}$ were injected subcutaneously into the hind footpad of C57BL/6J recipients. After 18 h, 3×10^5 CFSE-labelled *CD40lg*$^{SrtA/Y}$ CD4-Cre OT-II (or wild-type OT-II as control) CD4$^+$ T cells were transferred intravenously. PLNs were analysed by flow cytometry 72 h after T-cell transfer. Histograms show comparable expansion of both transferred T-cell populations, as indicated by CFSE dilution. Data are representative of two independent experiments.

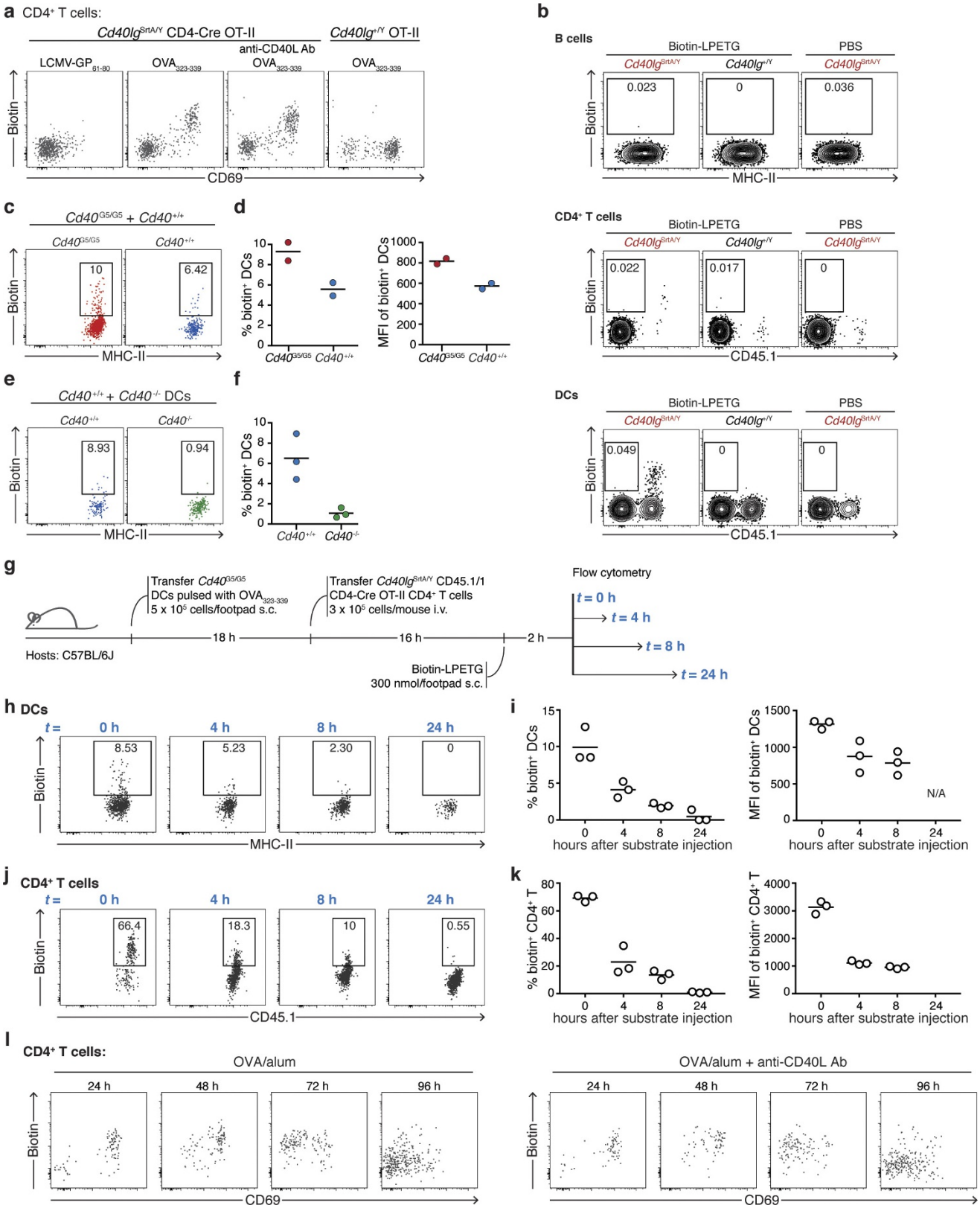

Extended Data Figure 7 | See next page for caption.

Extended Data Figure 7 | Characterization of LIPSTIC labelling *in vivo*. **a**, CD40L–SrtA expression in *Cd40lg*$^{SrtA/Y}$ CD4-Cre OT-II CD4$^+$ T cells *in vivo* after dendritic cell transfer. Mice were treated as in Fig. 3a. Flow cytometric analysis of PLN cells shows transferred *Cd40lg*$^{SrtA/Y}$ CD4-Cre OT-II CD4$^+$ T cells expressing CD40L–SrtA as revealed by the detection of biotin staining (formation of an acyl intermediate between SrtA and biotin–LPETG). CD40L–SrtA expression requires dendritic cell presentation of cognate antigen ($OVA_{323–339}$), is not affected by CD40L-blocking antibody treatment and positively correlates with the activation marker CD69. **b**, Detection background in major leukocyte populations. *Cd40*$^{G5/G5}$ CD45.1/2 dendritic cells were treated with $OVA_{323–339}$ and transferred subcutaneously (5×10^5 per footpad) into *Cd40*$^{G5/G5}$ recipients. After 18 h, 3×10^5 *CD40lg*$^{SrtA/Y}$ CD45.1/1 CD4-Cre OT-II (or *Cd40lg*$^{+/Y}$ CD45.1/1 OT-II lacking Cre expression as control) CD4$^+$ T cells were transferred intravenously. Biotin–LPETG (or PBS as control) was administered subcutaneously (300 nmol per footpad) 10 to 12 h after T-cell transfer and PLN cells were analysed by flow cytometry. Plots show biotin staining among B cells, CD4$^+$ T cells and dendritic cells. **c**, Efficiency of labelling of *Cd40*$^{G5/G5}$ and *Cd40*$^{+/+}$ dendritic cells after T cell–dendritic cell interaction *in vivo*. *Cd40*$^{G5/G5}$ and *Cd40*$^{+/+}$ dendritic cells were treated *ex vivo* with $OVA_{323–339}$, mixed and injected subcutaneously into C57BL/6J recipients (5×10^5 per footpad). After 18 h, 3×10^5 *Cd40lg*$^{SrtA/Y}$ CD4-Cre OT-II CD4$^+$ T cells were transferred intravenously. Biotin–LPETG was administered subcutaneously (300 nmol per footpad) 10–12 h after T-cell transfer. Dot plots show flow cytometric analysis of transferred *Cd40*$^{G5/G5}$ and *Cd40*$^{+/+}$ dendritic cells. **d**, Percentage (left) and MFI (right) of biotin$^+$ dendritic cells (gated as in **c**) among transferred dendritic cell populations. Labelling of *Cd40*$^{+/+}$ dendritic cells probably reflects biotin–LPETG transfer onto endogenous N-terminal glycines. Each symbol represents one mouse; bars indicate the mean. **e**, Labelling of endogenous N-terminal glycines requires CD40L–CD40 interaction. Experimental setup as in **c**, except that a mixture of C57BL/6J and *Cd40*$^{-/-}$ dendritic cells was transferred. Dot plots show flow cytometric analysis of transferred *Cd40*$^{+/+}$ and *Cd40*$^{-/-}$ dendritic cells. **f**, Percentage of biotin$^+$ dendritic cells gated as in **e** among transferred dendritic cell populations. Each symbol represents one mouse; bars indicate the mean. **g**, Graphic representation of the experimental protocol used in **h**–**k** to determine the clearance of surface biotin labelling. *Cd40*$^{G5/G5}$ dendritic cells were treated with $OVA_{323–339}$ and transferred subcutaneously (5×10^5 per footpad) into C57BL/6J recipients. After 18 h, 3×10^5 *CD40lg*$^{SrtA/Y}$ CD4-Cre OT-II CD4$^+$ T cells were transferred intravenously, biotin–LPETG was administered subcutaneously (300 nmol per footpad) 10–12 h after T-cell transfer. PLNs were collected and analysed by flow cytometry 0, 4, 8 or 24 h after the final biotin–LPETG injection. **h**, Flow cytometric analysis of PLN cells showing biotin labelling of transferred *Cd40*$^{G5/G5}$ dendritic cells at the indicated hours after biotin–LPETG administration. **i**, Percentage (left) and MFI (right) of biotin$^+$ dendritic cells among transferred *Cd40*$^{G5/G5}$ dendritic cells gated as in **h**. Each symbol represents one mouse; bars indicate the mean. **j**, Flow cytometric analysis of PLN cells showing biotin labelling of transferred *Cd40lg*$^{SrtA/Y}$ CD4-Cre OT-II CD4$^+$ T cells at the indicated time points after biotin–LPETG administration. **k**, Percentage (left) and MFI (right) of biotin$^+$ cells among transferred *Cd40lg*$^{SrtA/Y}$ CD4-Cre OT-II CD4$^+$ T cells gated as in **h**. Each symbol represents one mouse; bars indicate the mean. **l**, CD40L–SrtA expression in *Cd40lg*$^{SrtA/Y}$ CD4-Cre OT-II CD4$^+$ T cells *in vivo* after immunization. Mice were treated as in Fig. 3d. Flow cytometric analysis of PLN cells showing transferred *Cd40lg*$^{SrtA/Y}$ CD4-Cre OT-II CD4$^+$ T cells in mice left untreated (left) or treated with CD40L-blocking antibody 4 h before PLN collection (right). Data are representative of two independent experiments.

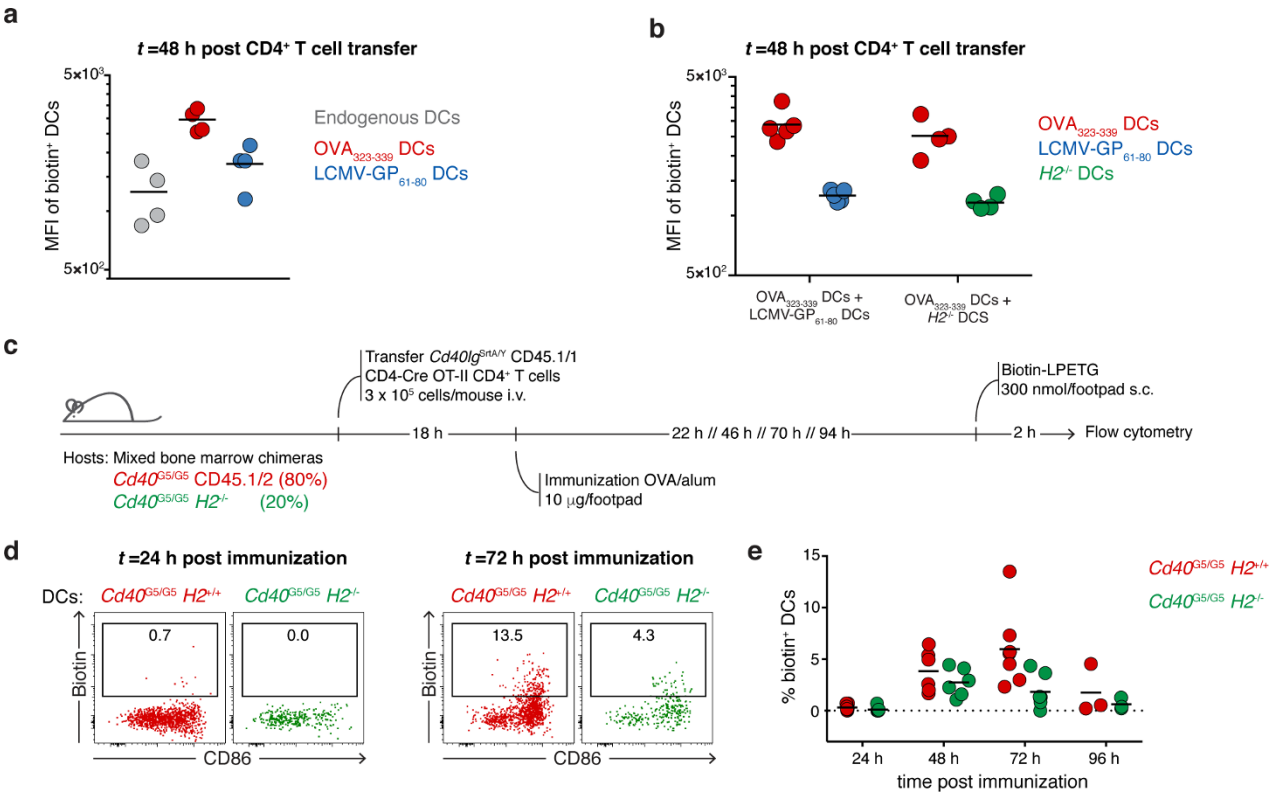

Extended Data Figure 8 | CD40–CD40L interaction between CD4$^+$ T cells and dendritic cells *in vivo* can occur in an antigen-independent manner. a, MFI of biotin$^+$ dendritic cells 48 h after T-cell transfer in mice treated as in Fig. 4a. Each symbol represents one mouse; bars indicate the mean. Data are pooled from two independent experiments. **b**, MFI of biotin$^+$ dendritic cells 48 h after T-cell transfer in mice treated as in Fig. 4d. Each symbol represents one mouse; bars indicate the mean. **c**, Graphic representation of the experimental protocol used in **d**, **e**. C57BL/6J mice were lethally irradiated and reconstituted with a mixture of *Cd40*$^{G5/G5}$ (80%) and *Cd40*$^{G5/G5}$;*H2*$^{-/-}$ (20%) bone marrow. After reconstitution, bone marrow chimaeras received 3×10^5 *Cd40lg*$^{SrtA/Y}$ CD4-Cre OT-II CD4$^+$ T cells intravenously and were immunized the following day with 10 μg of OVA in alum in the hind footpad. PLN were analysed 24, 48, 72 and 96 h after immunization. Biotin–LPETG was administered subcutaneously (300 nmol per footpad) during the last 2 h before analysis. **d**, Flow cytometric analysis of PLN cells showing biotin labelling of endogenous *Cd40*$^{G5/G5}$ and *Cd40*$^{G5/G5}$;*H2*$^{-/-}$ dendritic cells at 24 or 72 h after immunization. **e**, Percentage of biotin$^+$ dendritic cells among *Cd40*$^{G5/G5}$ and *Cd40*$^{G5/G5}$;*H2*$^{-/-}$ dendritic cells gated as in **d**. Each symbol represents one mouse; bars indicate the mean. Data are pooled from two independent experiments.

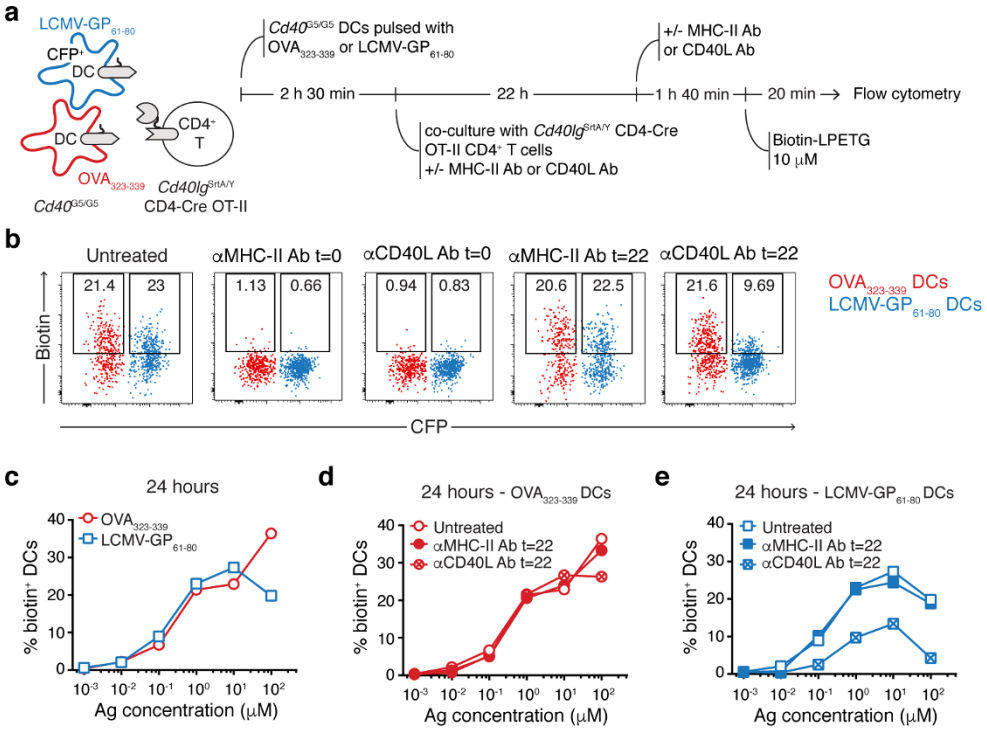

Extended Data Figure 9 | CD40–CD40L interaction between CD4$^+$ T cells and dendritic cells *ex vivo* can occur in an antigen-independent manner. a, Experimental setup used in **b**–**e**. Two *Cd40*$^{G5/G5}$ dendritic cell populations were individually treated with the indicated concentrations of either OVA$_{323–339}$ or LCMV-GP$_{61–80}$, mixed and co-cultured for 24 h with *Cd40lg*$^{SrtA/Y}$ CD4-Cre OT-II CD4$^+$ T cells. Biotin–LPETG was added during the last 20 min of co-culture at a final concentration of 10 μM, and cells analysed by flow cytometry. Where indicated, CD40L- or MHC-II-blocking antibodies were added at a final concentration of 150 μg ml^{-1} either at the beginning of co-culture ($t = 0$) or 2 h before analysis ($t = 22$). **b**, Flow cytometric analysis of dendritic cells treated with 1 μM peptides showing biotin labelling. **c**–**e**, Percentage of biotin$^+$ dendritic cells gated as in **b**. Data are representative of three independent experiments.

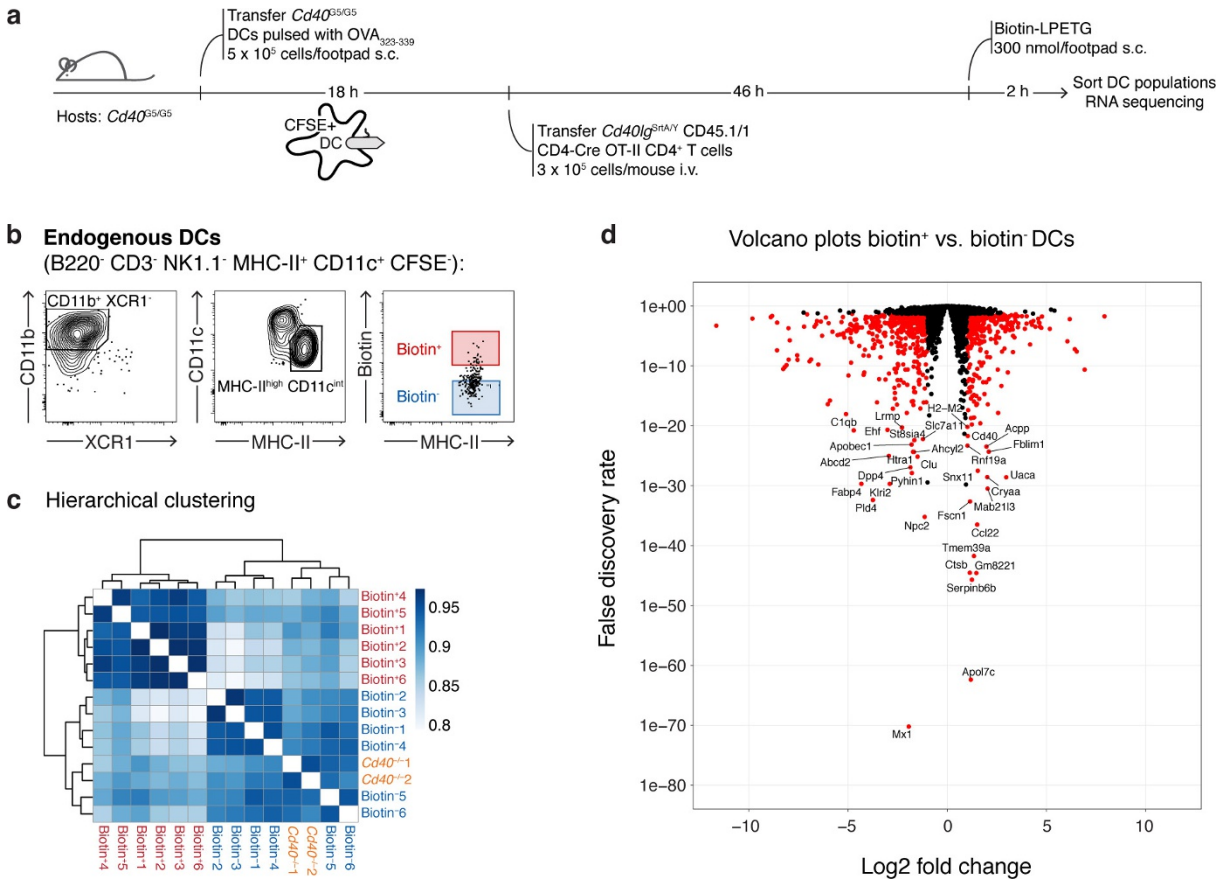

Extended Data Figure 10 | RNA sequencing analysis of sorted biotin$^+$ dendritic cells. a, Graphic representation of the protocol for dendritic cell sorting. Five hundred thousand *Cd40*$^{G5/G5}$ CFSE-labelled dendritic cells treated *ex vivo* with $OVA_{323–339}$ were injected subcutaneously into the hind footpad of *Cd40*$^{G5/G5}$ recipients. After 18 h, 3×10^5 *CD40lg*$^{SrtA/Y}$ CD4-Cre OT-II CD4$^+$ T cells were transferred intravenously. Biotin–LPETG was administered subcutaneously (300 nmol per footpad) during the last 2 h before analysis. PLNs were collected 48 h after T-cell transfer and dendritic cell populations were sorted by flow cytometry and later processed for RNA-sequencing analysis. As controls, dendritic cells were also sorted from *Cd40*$^{-/-}$ mice, which were treated as above except that they received wild-type (instead of *Cd40*$^{G5/G5}$) dendritic cells and wild-type OT-II (instead of *CD40lg*$^{SrtA/Y}$ CD4-Cre OT-II) CD4$^+$ T cells. **b**, Gating strategy for sorting. Endogenous dendritic cells were first identified as B220$^-$CD3$^-$NK1.1$^-$MHC-II$^+$CD11c$^+$CFSE$^-$. Sorting was restricted to CD11b$^+$XCR1$^-$ dendritic cells showing an activated phenotype (MHC-II^{hi}), which represent the major population involved in bystander interactions. Biotin$^+$ and biotin$^-$ dendritic cells were gated as shown. **c**, Hierarchical clustering of transcriptomic profiles. Colour scheme is based upon Pearson correlation. Data are derived from a single experiment, $n = 3$. **d**, Volcano plots showing differential gene expression between biotin$^+$ and biotin$^-$ dendritic cells. All genes used for the differential expression analysis are shown; differentially expressed genes ($\log_2$(fold change) > 1 and false-discovery rate < 0.05, see Methods) are coloured red. Data are derived from a single experiment, $n = 3$.

nature research

Corresponding author(s): Gabriel D. Victora

☐ Initial submission ☐ Revised version ☒ Final submission

Life Sciences Reporting Summary

Nature Research wishes to improve the reproducibility of the work that we publish. This form is intended for publication with all accepted life science papers and provides structure for consistency and transparency in reporting. Every life science submission will use this form; some list items might not apply to an individual manuscript, but all fields must be completed for clarity.

For further information on the points included in this form, see Reporting Life Sciences Research. For further information on Nature Research policies, including our data availability policy, see Authors & Referees and the Editorial Policy Checklist.

Experimental design

1. Sample size

Describe how sample size was determined.

We did not predetermine sample size. All experiments were performed multiple times and conclusions were considered valid if results were reproducible between experiments.

2. Data exclusions

Describe any data exclusions.

For FACS analysis of DCs in lymph nodes, low count samples (< 300'000 total events) where excluded due to the inability to clearly identify rare DC populations.

3. Replication

Describe whether the experimental findings were reliably reproduced.

All attempts at replication were successful.

4. Randomization

Describe how samples/organisms/participants were allocated into experimental groups.

Samples were not randomized. Donor mice were chosen based on their genotype. Recipient mice were allocated so that experimental and control groups were housed within the same cage.

5. Blinding

Describe whether the investigators were blinded to group allocation during data collection and/or analysis.

The investigators were not blinded to group allocation during experiments and outcome assessment.

Note: all studies involving animals and/or human research participants must disclose whether blinding and randomization were used.

6. Statistical parameters

For all figures and tables that use statistical methods, confirm that the following items are present in relevant figure legends (or in the Methods section if additional space is needed).

n/a	Confirmed
☐	☒ The exact sample size (*n*) for each experimental group/condition, given as a discrete number and unit of measurement (animals, litters, cultures, etc.)
☐	☒ A description of how samples were collected, noting whether measurements were taken from distinct samples or whether the same sample was measured repeatedly
☐	☒ A statement indicating how many times each experiment was replicated
☐	☒ The statistical test(s) used and whether they are one- or two-sided (note: only common tests should be described solely by name; more complex techniques should be described in the Methods section)
☐	☒ A description of any assumptions or corrections, such as an adjustment for multiple comparisons
☐	☒ The test results (e.g. *P* values) given as exact values whenever possible and with confidence intervals noted
☐	☒ A clear description of statistics including central tendency (e.g. median, mean) and variation (e.g. standard deviation, interquartile range)
☐	☒ Clearly defined error bars

See the web collection on statistics for biologists for further resources and guidance.

Software

Policy information about availability of computer code

7. Software

Describe the software used to analyze the data in this study.	Data were analyzed using Graphpad Prism 6 (graphing, statistical analysis) , FlowJo (flow cytometry) v.10.0.8, Metamorph (image acquisition) and ImageJ 1.50h (image analysis) and DESeq2 1.16.0 (RNAseq analysis).

For manuscripts utilizing custom algorithms or software that are central to the paper but not yet described in the published literature, software must be made available to editors and reviewers upon request. We strongly encourage code deposition in a community repository (e.g. GitHub). *Nature Methods* guidance for providing algorithms and software for publication provides further information on this topic.

Materials and reagents

Policy information about availability of materials

8. Materials availability

Indicate whether there are restrictions on availability of unique materials or if these materials are only available for distribution by a for-profit company.	Materials are available upon request.

9. Antibodies

Describe the antibodies used and how they were validated for use in the system under study (i.e. assay and species).	All antibodies used were commercially availalbe, and used only on species for which they have been validated by the vendor. Rat monoclonal anti-MHC-II BV421 (clone M5/114.15.2) BioLegend 107632 Rat monoclonal anti-MHC-II FITC (clone M5/114.15.2) BioLegend 107606 Rat monoclonal anti-MHC-II APC-Cy7 (clone M5/114.15.2) BioLegend 107628 Armenian hamster monoclonal anti-CD11c BV605 (clone N418) BioLegend 117334 Armenian hamster monoclonal anti-CD11c BV711 (clone N418) BioLegend 117349 Armenian hamster monoclonal anti-CD11c APC (clone N418) BioLegend 117310 Rat monoclonal anti-CD11b BV421 (clone M1/70) BioLegend 101236 Rat monoclonal anti-CD11b BV711 (clone M1/70) BioLegend 101242 Mouse monoclonal anti-XCR1 PerCP-Cy5.5 (clone ZET) BioLegend 148208 Mouse monoclonal anti-biotin PE Miltenyi Biotec 130-090-756 Rat monoclonal anti-CD3 PerCP-Cy5.5 (clone 17A2) BioLegend 100218 Rat monoclonal anti-CD3 APC-Cy7 (clone 17A2) BioLegend 100222 Rat monoclonal anti-B220 APC-Cy7 (clone RA3-6B2) BioLegend 103224 Rat monoclonal anti-NK1.1 APC-Cy7 (clone PK136) BioLegend 108724 Rat monoclonal anti-CD169 PE-Cy7 (clone 3D6.112) BioLegend 142412 Rat monoclonal anti-F4/80 PE-Cy7 (clone BM8) BioLegend 123114 Rat monoclonal anti-Ly6c PerCP-Cy5.5 (clone HK1.4) BioLegend 128012 Armenian hamster monoclonal anti-CD69 BV421 (clone H1.2F3) BioLegend 104528 Armenian hamster monoclonal anti-CD40L APC (clone MR1) BioLegend 106510 Armenian hamster monoclonal anti-CD40L biotin (clone MR1) eBioscience 13-1541-82 Rat monoclonal anti-CD4 PE-Cy7 (GK1.5) BioLegend 100422 Rat monoclonal anti-CD4 APC (GK1.5) BioLegend 100412 Rat monoclonal anti-CD4 PerCP-Cy5.5 (GK1.5) BioLegend 100434 Mouse monoclonal anti-CD45.1 FITC (A20) BioLegend 110705 Mouse monoclonal anti-CD45.1 BV711 (A20) BioLegend 110739 Mouse monoclonal anti-CD45.1 AF700 (A20) BioLegend 110724 Mouse monoclonal anti-CD45.1 PE-Cy7 (A20) BioLegend 110730 Rat monoclonal anti-CD86 BV605 (GL1) BioLegend 105037 Rat monoclonal anti-Igk PE (clone 187.1) BD Biosciences 559940 Armenian hamster monoclonal anti-CD40L (clone MR1) BioXCell BE0017-1 Rat monoclonal anti-MHC-II (clone M5/114) BioXCell BE0108 Rat monoclonal anti-CD40 (clone 1C10) Biolegend 102810 Rabbit polyclonal anti-FLAG tag Sigma F7425 Mouse monoclonal anti-c-Myc tag (clone 9E10) Thermo-Fisher Scientific 13-2500 Rabbit monoclonal anti-a-Tubulin HRP (clone 11H10) CST 9099 Streptavidin HRP Jackson ImmunoResearch 016-030-084 Goat polyclonal anti-rabbit IgG HRP Cell Signaling Technology 7074P2 Goat polyclonal anti-mouse IgG1 HRP Southern Biotech 1070-05

10. Eukaryotic cell lines

a. State the source of each eukaryotic cell line used.
All cell lines were from ATCC.

b. Describe the method of cell line authentication used.
Cell lines were not authenticated in our laboratory.

c. Report whether the cell lines were tested for mycoplasma contamination.
All cell lines tested negative for mycoplasma contamination.

d. If any of the cell lines used are listed in the database of commonly misidentified cell lines maintained by ICLAC, provide a scientific rationale for their use.
No commonly misidentified cell lines were used.

Animals and human research participants

Policy information about studies involving animals; when reporting animal research, follow the ARRIVE guidelines

11. Description of research animals

Provide details on animals and/or animal-derived materials used in the study.
C57BL6/J, Ptprca, Cd40-/-, Cd40lg-/-, H2-/-, CD4-Cre transgenic and ECFP-transgenic mice were purchased from The Jackson Laboratory (strain numbers 000664, 002014, 002928, 002770, 003584, 022071 and 004218, respectively). Cd40G5 and Cd40lgSrtA mice were generated and maintained in our laboratories. IghB1-8hi and OT-II transgenic (Y chromosome) mice were originally provided by M. Nussenzweig (Rockefeller University, New York, USA). Males and female mice, 5-12 week-old, were used in all experiments.

Policy information about studies involving human research participants

12. Description of human research participants

Describe the covariate-relevant population characteristics of the human research participants.
The study did not involve human research participants.

nature research

Corresponding author(s): Gabriel D. Victora

☐ Initial submission ☐ Revised version ☒ Final submission

Flow Cytometry Reporting Summary

Form fields will expand as needed. Please do not leave fields blank.

Data presentation

For all flow cytometry data, confirm that:

☐ 1. The axis labels state the marker and fluorochrome used (e.g. CD4-FITC).

☐ 2. The axis scales are clearly visible. Include numbers along axes only for bottom left plot of group (a 'group' is an analysis of identical markers).

☐ 3. All plots are contour plots with outliers or pseudocolor plots.

☒ 4. A numerical value for number of cells or percentage (with statistics) is provided.

Methodological details

5. Describe the sample preparation.	Popliteal lymph nodes were harvested, incubated 30 min at 37 °C in RPMI, 2% FBS, 20 mM Hepes, 400 U/ml type 4 collagenase (Worthington Biochemical Corporation), disrupted using disposable micropestles (Axygen) and filtered through a 70 µm cell strainer. Single-cell suspensions were washed with PBS, 0.5% BSA, 2mM EDTA (PBE), incubated at RT for 5 minutes with 1 µg/mL of anti-CD16/32 (2.4G2, BioXCell) and then stained for cell surface markers at 4 °C for 15 min in PBE using the reagents listed in Supplementary Table 3. Cells were washed with PBS and stained with Zombie fixable viability dyes (Biolegend) at RT for 15 min and then fixed with Cytofix (BD Biosciences) before acquisition. In all in vivo experiments involving detection of Biotin-LPETG SrtA substrate, anti-biotin PE antibody (Miltenyi Biotec) was exclusively used due to its lower background compared to Streptavidin conjugates.
6. Identify the instrument used for data collection.	Samples were acquired on Fortessa or LSR-II flow cytometers (BD Biosciences).
7. Describe the software used to collect and analyze the flow cytometry data.	Samples were acquired using Diva software (BD Biosciences) and data were analyzed using FlowJo v.10.0.8 software.
8. Describe the abundance of the relevant cell populations within post-sort fractions.	The abundance of the relevant cell population in the post-sort fraction was not assessed.
9. Describe the gating strategy used.	DC analysis: DCs were identified as Zombie-, B220-, CD3-, NK1.1-, MHC-II+, CD11c+, F4/80- CD169-. CD4+ T cells analysis: CD4+ T cells were identified as Zombie-, MHC-II-, CD4+.

Tick this box to confirm that a figure exemplifying the gating strategy is provided in the Supplementary Information. ☐